MODEL PREDICTIVE CONTROL FOR LOAD FREQUENCY CONTROL OF AN INTERCONNECTED POWER SYSTEM

By

Igbineweka Ernest Uyioghosa

219087713

A dissertation submitted in partial fulfillment of the requirements for the degree

Of

Master of Science in Electrical Engineering

College of Agriculture, Engineering and Science, University of KwaZulu-Natal

2019

Supervisor: Dr. A. Saha

CERTIFICATION

As the candidate's Supervisor, I agree to the submission of this dissertation.

Signed: _____

Dr. A Saha

DECLARATION 1 – PLAGIARISM

I, Igbineweka Ernest Uyioghosa declare that:

1. The research reported in this thesis, except where otherwise indicated, and is my original research.
2. This thesis has not been submitted for any degree or examination at any other university.
3. This thesis does not contain other persons' data, pictures, graphs or other information unless specifically acknowledged as being sourced from other persons.
4. This thesis does not contain other persons' writing unless specifically acknowledged as being sourced from other researchers. Where other written sources have been quoted, then:

a) Their words have been re-written, but the general information attributed to them has been referenced

b) Where their exact words have been used, then their writing has been placed in italics and inside quotation marks and referenced.

5. This thesis does not contain text, graphics or tables copied and pasted from the Internet, unless specifically acknowledged, and the source being detailed in the thesis and in the References sections.

Signed: _____

Igbineweka Ernest Uyioghosa

DECLARATION 2 – PUBLICATIONS

The work in this dissertation has been submitted to the Southern African universities power engineering conference (SAUPEC). The details are as follows:

Igbineweka E. Uyioghosa, A. K. Saha, "A comparative analysis of different MPC controllers for load frequency control for interconnected Power System", SAUPEC 2020, January, Cape Town.

Igbineweka E. Uyioghosa, A. K. Saha, "DMPC scheme on load frequency control with application to interconnected power system", SAUPEC 2020, January, Cape Town.

Signed: _____

Igbineweka Ernest Uyioghosa

ACKNOWLEDGEMENTS

Firstly, I want to appreciate God almighty for his preservation, provision, and protection for the opportunity given to me to carry out this research. Also, many thanks to my supervisor, Dr. A.k. Saha, for your training, teaching, encouragement, for your prompt reply to my email, and also for providing me with this research topic

I am greatly indebted to my siblings particularly, for their invaluable support, encouragement and most importantly, understanding during this research. To my friends, you ignited my passion to make a difference by furthering my studies. I will never be able to articulate what I felt since I met you all. You all, remain the best.

Lastly, to my number one fan, my mum Mrs. Roseline Igbineweka, who imparted in me the spirit of resilience, that people say I operate with, I say, thank you for the love, sacrifice and letting me do all that I was created to do. I am still working very hard. I will not lower my guard, I will not let you down. From the depth of my heart, I say, thank you.

DEDICATION

This dissertation is dedicated to my lovely mum Mrs. Igbinweka Roseline.

ABSTRACT

Reliable load frequency control (LFC) is of importance in modern power system generation, transmission and distribution, it has been the basis of research on advanced control theory and application in recent years. In LFC scheme, local load disturbance, inter-area ties power fluctuation, frequency deviation, generation rate constraints (GRC), and governor dead band (GDB) are the major nonlinear factors on the control scheme that affect the dynamic response of the system to a large extent. Over the years, many methods have been designed for LFC problem of which model predictive controller (MPC) stands out due to its advantages. MPC is a control approach that simulates the feature behaviour of a system it controls and based on the result of the simulation attempt to find a control output such that the simulated system behaves optimally. When applied to LFC it copes with the perturbation.

In this dissertation, robust distributed model predictive control (RDMPC) is developed as a controller scheme for LFC and is compared with a proportional integral derivative (PID) controller using MATLAB/Simulink for two-area and three-area hydro-thermal interconnected power system. From the simulation result, RDMPC significantly shows robustness over PID when compared in frequency deviation and area control error. It is observed that RDMPC still lags, from system varying dynamics and uncertainty despite its robustness over PID, hence an adaptive model predictive control (AMPC) is developed to improve on the performance of RDMPC. In order to evaluate the efficacy of this proposed controller, robustness and comparative analysis is performed using MATLAB/Simulink between the conventional PID, RDMPC, and AMPC with respect to performance indices such as settling time, undershoot and peak overshoot when subjected to frequency deviation, tie-line active power deviation, and area control error. Also, the dynamic response of the hydrothermal systems is analysed and compared in the presence of nonlinear constraints such as generator rate constraint (GRC) and governor dead band (GDB). The result from the simulation tests shows that AMPC has a better dynamic response when compared with PID, and RDMPC with a significant improvement.

TABLE OF CONTENTS

LIST OF FIGURES

LIST OF TABLES

LIST OF ABBREVIATIONS

ACE	Area Control Error
AGC	Automatic Generation Control
AMPC	Adaptive Model Predictive Control
CA	Control Area
Ce-MPC	Centralized Model Predictive Control
De-MPC	Decentralized Model Predictive Control
DMPC	Distributed Model Predictive control
GA	Genetic Algorithm
GDB	Generator Dead Band
GRC	Generation Rate Constraint
GPC	Generalized Productive Control
IPS	Interconnected Power System
LFC	Load Frequency Control
LTI	Linear Time Invariant
LMI	Linear Matrix Inequality
MPC	Model Predictive Control
PI	Proportional-Integral
PID	Proportional-Integral-Derivative
RDMPC	Robust Distributed Model Predicative control
SVD	Singular Value Decomposition
SMC	Sliding Mode Control

CHAPTER 1

INTRODUCTION

1.0 Background of study

Power systems as seen in different countries are made up of two or more generating and distribution power systems. These large power systems consist of interconnected power subsystems covering wide geographical control areas (CA) [1]. Each of these subsystems has different generating capabilities with variable load demands. The control of power flow between these areas is through the tie-lines. Since these several subsystems and the control areas are linked together, the load disturbance and load demand change in an area can alter the output frequencies of other interconnected areas including power flow on the tie-line [2]. The real-life behaviour of power systems shows that there are always load dynamic issues having to do with load changes especially dealing with the rate of change. Load frequency controllers (LFC) are used to sense these perturbations and to achieve mismatch corrections by balancing the mismatch between the frequencies and tie-lines active power of the interconnected [3]. Extensive research has been conducted on LFCs control algorithms and methodologies, it is still ongoing to efficiently and optimally manage these load perturbations and keep the steady-state errors to zero amongst other constraints, which has resulted in the development of several techniques for LFC problem [4].

The well-known traditional technique use for the LFCs is either proportional-integral (PI) or proportional integral derivative (PID) controllers with other variants exist that aid in the proper tuning of their parameters. Using PIDs fall short due to the inability of handling uncertainties and non-linear constraints [1,5]. Several robust control design strategies have been applied to solve the LFC problem and to improve its ability to deal with power plant uncertainties. Varieties of robust control designs exist, which include adaptive feedback policies based robust control [6] and adaptive robust control [7], decentralized robust control using iterative linear matrix inequalities (LMIs) [8], decentralized control [9], etc. Several popular control methodologies that have gained attention in decentralized LFC of multi-area power systems include a model predictive controller (MPC), sliding mode control (SMC) [10], and singular value decomposition (SVD) [11], etc. Intelligent techniques have also been applied in LFC design. The basic PID controller parameters have been worked upon by different researchers using various global optimization techniques involving evolutionary and swarm intelligence to tune the parameters for improved robust performance. The Genetic algorithm (GA) has been used in the LFC design to

achieve a variable structure controller in [12,13]. Fuzzy logic-based gain scheduling has been used in [14], to achieve a better control strategy for LFC. The authors in [14,15], investigated the application of neural networks in the LFC problem solution. Bacterial foraging algorithm [16], fuzzy logic [17], recurrent fuzzy neural network [18], are examples of other intelligent algorithms that have also been applied in LFC for interconnected power systems(IPS). Some of these techniques exhibit implementation simplicity with a better dynamic response but suffer performance deterioration due to increased load disturbances and boiler dynamics that accompany increasing power system complexities [19,20]. Some controllers have poor performance because their tuning is based on a trial-error approach [3]. Some controllers can handle some constraints at a time but fail when it comes to multi-objective controls. A peculiar problem with the intelligence-based techniques of [16,17] and [18,21], is that they have too many computational algorithms that involve a large computational burden with an implication of slow response time and too much hardware resources.

Over the past decades, MPC technique and its variants have stood out due to its advantages that include its straightforward formulation, based on well-understood concepts, can handle multi-objective controls, explicitly handling of constraints including input saturation constraints, can handle control of parameters and constraints over wide operating range [6,22], and have been successfully implemented in LFC and process industries. When modelling power systems for analysis, the entire system has multiple inputs and multiple controlled outputs. A system that exhibits complex and multi-variable interactions between inputs and outputs variables is needed to operate within operating constraints [23]. MPC fits these model characteristics that can explicitly work with constraints including input saturation constraints and product quality constraints. Its development time when compared with other advanced control methods is much shorter and can handle multiple inputs, multiple controlled outputs, and constraints [23,24].

MPC is unique as it can systematically handle multivariable interactions, operating constraints, and process nonlinearity. It is the second most used multivariable control scheme in the process industries over the last four decades for critical unit operations like reactors used in refineries with increasing computing power. MPC is increasingly finding applications in diverse areas such as in fuel cells, robotics, automation, internet search engines, biomedical applications, planning, scheduling and control of drives, [23,24].

MPC, make use of optimization techniques, utilizes a model of the system to forecast system behaviour by optimizing the system output to produce the best optimal control result at the current time instance [2,3]. MPC was first used in the process industries, a lot of useful MPC industrial applications have been put into operation in the same industries [4]. Recent studies have been focused on the MPC's area of application, for the control of smart industrial systems. Since

modern power are increasing in size, conventional MPC are becoming less reliable, the set back of this MPC controllers result in the advancement of different MPC controllers. Several variants of MPC have been created and researched since its inception as applied to LFC. They include the following;

1. Decentralized model predictive based LFC
2. Centralized model predictive LFC
3. Robust distributed model predictive LFC

MPC in its basic implementation is a centralized pattern. The controller has the complete details of the system and calculates all the control inputs and states for the system, hence the Centralized MPC (Ce-MPC) system is a de-facto standard of MPC algorithm that all other variants of MPC are measured against or compared with [25]. However, Ce-MPC controllers are viewed by most power system players as impractical when it comes to large power systems as we have them today for the following reasons;

1. Most MPC practitioners consider Ce-MPC as monolithic and inflexible because of its structure.
2. Ce-MPC controllers for large power systems will usually mean they have to deal with a large volume of data processing, and no one wants to deal with systems with too large data collection. Up to date, there exists no operational centralized control system for any large interconnected networked system.
3. The various large interconnected networked system is already in decentralized structure hence the implication of complete system overhaul and redesigns in other to implement centralized MPC is too much for operators and personnel.
4. All large power systems using MPC are all operating the decentralized MPC algorithms and their infrastructures have been set up to work with it and it will be difficult to implement a centralized system that could lead to complete system overhaul and that will cost inhibitive for any investor or practitioner.

Due to the hurdles of implementing Ce-MPC, then the goal of the decentralized MPC (De-MPC) algorithm is developed to work with existing control infrastructure, such that distributed MPC can be developed and improved upon to approach the advantages of the centralized MPC while having the advantages of being a distributed MPC system. To achieve this, De-MPC models influence or interact with other interconnected subsystems, information are shared and fed into the local subsystem, whereby allowing the local controllers of other interconnected subsystems to determine suitably their own feedback action that accounts for the external interactions [25]. The goal is that this additional information factored into the optimal solution will help improve

system-wide control performance [26]. Despite this feature, the De-MPC suffers from online applications due to speed of response due to delay caused by computational burden hence other robust MPC controllers were developed such as distributed MPC (DMPC), Robust distributed MPC (RDMPC), and an adaptive MPC (AMPC).

This work is focused on developing AMPC algorithm to improve the performance of RDMPC strategies for handling dynamic responses and uncertainties for LFC. When applied to two-area and three-area hydro-thermal interconnected power systems, in the presence of load disturbance, parameter deviation, and nonlinear constraint such as (GRC and GDB), conventional PID controller is used to compare these controllers to validate their robustness.

1.1 Motivation

The goal of power system generation and control is maintaining a reliable supply of power from the generating plant to the consumer (load) [1]. The modern power system comprises different power plants linked by tie lines. In a situation where there is a sudden load deviation from its nominal operating value, this leads to a sudden change in the system frequency which in turn lead to unwanted result across the different CA [26]. Hence LFC scheme is used to control the system by normalizing the system frequency to keep the tie line active power and ACE at its nominal value.

MPC makes use of optimization techniques, utilizes a model of the system to forecast system behaviour by optimizing the system output to produce the best optimal control result at the current time instance [4, 5, 6]. When applied to LFC, it gives a good optimal response by reducing steady-state error deviation, tie-line, area control error (ACE) and active power. One other objective is to keep the power supply constant without any disruption or voltage drop when it is being distributed to the consumers. As power system size increases geographically, utilities and interconnected power sources and MPC are becoming less reliable, this has led to the advancement of robust MPC controllers. A conventional controller (PID), a robust DMPC controller (RDMPC) and a more recent advance AMPC controller (AMPC), are discussed in this dissertation for LFC control for two-area and three-area hydro-thermal power system.

Although the design of AMPC schemes is very challenging for power system due to the assumption of the separation principle widely utilized in linear control systems is inapplicable to the general category of nonlinear systems [25]. To meet up with the need for a highly competitive economic market; engineers are striving constantly to raise performance limits in power system generation, distribution, and transmission. To eliminate the difficulty in the implementation of AMPC is the introduction of expanded state vector with optimization of control signal vector in the controller to effectively control LFC. The aim of this dissertation is to

develop AMPC algorithm with assured improvement over RDMPC, capable of approaching closed-loop stability [25,26]. The current state of AMPC research is another motivation as few available AMPC formulations for the control of LFC for power systems are based on novel literature assumptions.

1.2 Problem statement

A distinguishing feature between De-MPC and DMPC is the information exchange and interactions between a subsystem and other neighbouring subsystems [25]. This interaction greatly improves distributed over decentralized but there exists the problem whereby in order to satisfy conditions for stability, there is the tendency to increase information exchange rates as the system gets to equilibrium and sometimes leads to increasing prediction horizon which in turn may lead to instability.

For most coordinated and DMPC strategies in current literature, the applicability of MPCs in power systems is still limited due to computational burden and delay response to transient conditions which do lead to system instability. Added to this fact is an assumption in most DMPC formulations of having knowledge of the system state's feedback with the exclusion of cases involving local measurement estimation of each subsystem state. These formulations also assume that the plant parameters are fixed during operation which is not the case in real life as they change with change in operating conditions [26]. In this dissertation RDMPC with LMI formulations has been used to reduce computational burden for LFC for an IPS and to improve on system robustness. AMPC algorithm is developed to improve its speed of response for effective tracking of parameter change dynamics that improve online applications in LFC.

1.3 Aim and objectives

The aim of this dissertation is the design and simulation of an adaptive model predictive control for load frequency control for an interconnected power system. A system aimed at controlling load frequency controllers against power system disturbances, nonlinear constraints like generator rate constrain and governor dead band using proportion integral derivative, robust distributed model predictive control and adaptive model predictive methodology for two-area and three-area hydro-thermal interconnected power systems.

The objectives of this research include the following

1. Study and identify LFC controller problems of interconnected power systems.
2. Develop mathematical and models for LFC problems.

3. Develop models to represent different power system constraints like GRC in generated, and load change disturbance.
4. Develop a model of RDMPC and AMPC algorithm.
5. Implementation of RDMPC and AMPC model expressions for two-area and three-area hydro-thermal system.

The work objectives are achieved through the following questions:

1. What are the problems affecting LFC controllers in interconnected power systems?
2. What are the nature and characteristics of these LFC problems?
3. Are there techniques and methodologies employed to tackle these LFC problems and what are these methodologies?
4. What are the advantages of MPC methodologies that make it stand out in comparison with other methodologies in industrial applications?
5. How will the application of MPC methodologies tackle LFC problems in interconnected power systems?

1.4 Scope of work

In this research work, simulation test and analysis is carried out using MATLAB toolbox and MATLAB LMI Solver on two-area and three-area hydro-thermal system in order to evaluate the performance of these controllers which includes robustness test and comparative analysis between traditional PID, RDMPC and AMPC controller schemes, considering the performance indices like settling time, undershoot and peak overshoot of the response of the plant systems under load disturbances, system parameters and nonlinear constraints like GRC and GDB.

1.5 Organization of dissertation

This dissertation remaining chapters are organized as follows:

Chapter 2 is on the review of related literature from researchers on different MPC structures with more emphasis on DMPC. The inadequacies of some selected MPC structures are discussed leading to the motivation for RDMPC and AMPC algorithms proposed in this research.

Chapter 3 discusses the various MPC algorithms and their structures with more emphasis on the distributed MPC and RDMPC with their mathematical expressions.

Chapter 4 presents the proposed RDMPC for an optimization problem, with formulation resolved with linear matrix inequalities to guarantee closed-loop stability. The RDMPC is presented with tests and results for performance comparison with the traditional PID controller.

Chapter 5 presents the performance improvement of the RDMPC result to include an observer system with state estimation to achieve an adaptive MPC algorithm and the strategy is described.

Chapter 6 conclusion is made from the results and recommendations for future work are presented.

The notation used in the dissertation

The regular letter in italics represent scalar quantities while the bold italics symbols denote vectors/matrices. A^*, $|A|$,$\|A\|$, A^T, and Σ represent complex conjugate of a number, Euclidean norm, Frobenius norm, transpose, and summation respectively. While (…) represent Ellipsis, $\mathbb{R}$ is Mathbb, $A'(x)$ represent the derivative of the function A at the point x, ∂ is partial derivative, ∞ is infinity, and $\bar{A}$ represent the complex conjugate of A.

CHAPTER 2

LITERATURE REVIEW

2.0 Model predictive control

MPC algorithm has become one of the most accepted process control technology nowadays even with system process constraints handling, because of its increasing applicability in the multivariable process. This has resulted in MPC being applied in different industrial control processes [27,28]. Applications of MPC in industries ranging from chemical process control, robotics, and automation systems to LFC control in power plants, etc. [29,30].

The MPC and its variants at using the concept of process modelling and that of optimal open-loop feedback policy. The process modelling of MPC uses a dynamic model to generate a prediction for future subsystem behaviour, sort solution for its optimal control steps by minimizing an upper bound for objective function based on its prediction output trend. It takes previous measurements for each time step, takes input and outputs data to determine the current state and then applies the optimization solution to get the best optimal open-loop feedback law from the estimated state. The first input action of the input signal is the only one injected into the plant. The system's next state for the next step time frame is recalculated using new obtained values. The optimal open-loop policy is recalculated once the optimization problem is resolved. MPC methodology concept is presented in Figure 2-1.

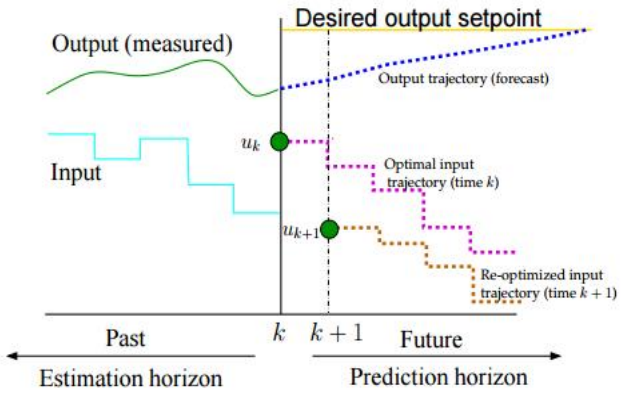

Figure 2-1 MPC methodology conceptual picture [31,32].

MPC uses the process model for each control time interval, carryout prediction of the plant output behaviour over the prediction horizon. It continues minimizing subsystem objective function in order to obtain a set of control actions to take over the entire control horizon. Only the first set of values of *uk* computed control moves are applied into the process and the entire computation is re-run with the next control interval *uk+1* to get the process feedback values [32]. Step response, transfer function, impulse response, and state-space models either continuous or discrete are types of linear models that can be applied in MPC algorithms. The use of linear and quadratic objective function depends on MPC algorithm, linear objective is mostly used because of good error averaging properties, it's simple, has a clear analytical solution which is easily obtained for the control without constraints, but quadratic programming use handles constrained control cases better [32]. Over the past four decades, MPC control structures have evolved into the following major MPC structures for the control of LFC;

1. Centralized model predictive control
2. Decentralized model predictive control
3. Distributed model predictive control

A lot of research work has been done and still ongoing with respect to the application of all the structures and expanding their algorithm to achieve the best control for applications. This work lays more emphasis on distributed MPC and application of adaptive control to give a better possible performance as Ce-MPC is not practical and De-MPC lacks the coordination as obtainable in an interconnected power system. This has led the trend that process industries are making a gradual shift from the decentralize PID control methodologies into a more centralized version by adopting a control structure called the distributed control system.

Despite the merit of De-MPC applications including lesser computations, close-loop performance still has some limitations because the individual MPC controllers in the structure subsystems operate in a decentralizing manner. The inter subsystems interactions are ignored and do result in the controller's instability especially when there are strong interactions. Researchers over the years have proposed several solutions to this problem by proposing other forms of controllers for the different subsystems so that they can exchange information through dedicated communication lines. Nash equilibrium-based coordination strategies [33], and weighted cost functions coordination-based schemes [32], have been reported. They present different information exchange structures and strategies that describe the information transfer between the subsystem's controller [34]. Each MPC in a decentralized system accesses only its own local objectives and solves its local cost function using its own controlled variables and does not take that of other subsystems into consideration. Coordinated MPC operation is the reverse in that while computing its objective function includes the interactions of other neighbouring subsystems using interactive

models and information sharing and by combining the shared solutions from other subsystems into its own local minimization problems thereby achieving a global objective. DMPC is a typical example of a coordinated MPC. It has better flexibility in relation to decentralized structure and having a performance that is close to Ce-MPC as it takes interactions for other subsystem processes into account [32].

The comprehensive research conducted in some literature from other researchers has led to the observation that there are two major issues in DMPC research discussed by [35], and [36]. The authors in [36], discussed DMPC technology challenges, they pointed out that robustness issues in developing DMPC is very important and should be addressed so that RDMPC strategies can work as expected. An author in [36], made some recommendations based on the comprehensive review they did on DMPC methodologies with respect to analytical tools developed to help attain a suitable optimal trade-off between MPC structure simplicity and system performance. The subsequent sections discussed a review of some DMPC strategies with LMI and AMPC.

2.1 Distributed model predictive control.

The authors in [37], have discussed extensively on the benefits of subsystems coordination, cross-integration requirement for MPCs. The authors in [38], presented a proposition that works based on a master-slave paradigm to develop a two-level decomposition coordination strategy for generalized predictive control (GPC). In [39,40], a plant-wide control strategy was presented, that involves the integration of linear and nonlinear MPC in a DMPC design framework, especially for controlling those systems whereby each subsystem dynamics is disconnected but their control variables and local state are non-separable but factored into the objective function. In [41], optimal input trajectories are computed by each subsystem for itself and neighbours with stability conditions well established. The authors in [41], pointed out that there are consequences to the stability condition proposed and they are: To satisfy stability condition, it would require high information exchange rates especially as it tends towards an equilibrium which is counter-productive in the long run and instability issues involved in increasing the prediction horizon as closed-loop performance tend to deteriorate beyond certain horizon points.

The authors in [42], proposed a continuous-time DMPC framework for the stabilization of a multi-vehicle formation with global feasibility. The author claims that there is an assurance of stability if compatibility constraint is used that will allow the subsystem responses to remain within specifying bound. A good degree of conservatism is introduced by the compatibility constraint but may lead to a response that is unlike that of Ce-MPC optimal performance. If based on this the compatibility constraint is relaxed it will lead to increase information exchange frequency to guarantee stability among the subsystems. This is a consequence of the author's claim that each

subsystem dynamics is decoupled, and that neighbour's states are only what will affect the local subsystem stage cost.

An unconstrained, linear time-invariant (LTI) systems based distributed MPC algorithm whereby the states of interacting subsystems affect the dynamics of other subsystems were presented in [43,44]. For each subsystem, they employed a contractive state constraint for each subsystem's MPC optimization with asymptotic stability will be guaranteed if the system satisfies a matrix stability condition. The work of [45], presents a framework for unconstrained DMPC for plant partitioning into properly sized subsystems. In any case properties like optimality, convergence and closed-loop stability were not established.

The literature in [46], describes a DMPC strategy, whereby interacting subsystem's effects were treated as bounded uncertainties. In this algorithm, a subsystem MPC is meant to solve the min-max optimization problem to determine which local control policy to apply. Though they proved system feasibility, closed-loop stability and optimality properties were unclear in their formulation.

For most available DMPC methodologies, nominal properties like optimality, feasibility, and closed-loop stability for any single DMPC framework have not been established and most assume perfect knowledge of state feedback and cases of subsystem states estimation from local measurements are not addressed. Based on all the DMPC reviewed, a robust DMPC algorithm is developed in chapter 4, using LMI for the optimization of LFC.

The author in [44], describe the DMPC scheme for LFC for the three-area power system, the dynamics model of the power system was introduced, MATLAB simulation results show that for load-displacement dynamic response of DMPC was better compared to conventional MPC. As most MPC literature has been focused on system dynamic response to load disturbances parameter uncertainty and nonlinear constraint, no much work is being done to investigate the effect of multiple load disturbance as real-life power plants are subjected to multiple variations of load. In this dissertation, a simulation is done on multiple load disturbances in chapter 5 in other to investigate the effectiveness of the dynamic response of the proposed controller to match online behaviour.

2.2 Robust control with linear matrix inequalities (LMIs)

A linear modelling design approach is mostly used in MPC design in most industrial applications. The presence of system nonlinearity model mismatch of inaccurate model identification makes using a linear modelling approach less accurate [47,48]. Nonlinear MPC can only provide partial mitigation of this problem because of application limitation arising from difficulty to design

nonlinear MPC for performance, stability and based on this nonlinear, in this research the power system used is linearized.

It is important to note that MPC make use of sensitivity to model uncertainties and mismatch, so that feedback control must be designed for good performance with robust control to account for model errors, robust control strategies are designed to explicitly input plant-model mismatch and other possible errors in the system design even going as far as representing all possible source of uncertainties [27,49]. There are research works that have been published on robust MPC, but explicit robustness of distributed MPC strategies is still lacking.

LMI is used in RDMPC design to deal with the supposed computational complexity arising from modelling errors for robustness control purposes [27,50]. This feature of LMI efficiently addresses matrix inequalities by employing efficient interior-point methods resulting in polynomial time solutions makes it very attractive and leads to improved speed of RDMPC strategy. There are special LMI solvers software like that in MATLAB and an integrated YALMIP design as well as other solvers [51], used for formulating many convex LMI problems. Authors in [52], present comprehensive literature on LMIs maths, similar in [53], the literature providing LMI's concepts and applications. LMI's control design and synthesis are presented as follows:

$$F(x)=F_0+\sum_{i=1}^{N} x_i F_i > 0 \tag{2.1}$$

where F_i is real n × n matrices and they are symmetrical, x_i is a variable and $F(x) > 0$ is positive definite. LMI can be used to three main problems and they are

1. The feasibility problems.
2. The linear programming problems.
3. Generalized minimization of eigenvalue problems.

This is in addition to the fact that it can plant model uncertainty explicitly, the core of algebraic manipulations for LMI formulation is the Schur complement lemma which is an attractive way for solving complex problems. Schur lemma is reviewed briefly as it plays a vital role in current research work. Let examine the convex nonlinear inequalities presented:

$$R(x)> 0,\ Q(x)- S(x) R(x)^{-1}S(x)^{T} > 0 \tag{2.2}$$

$Q(x) = Q(x)T$, $R(x) = R(x)T$ *and* $S(x)$ all depend on x. Application of Schur complement will convert (2.2) to the equivalent LMI presented as

$$\begin{bmatrix} Q(x) & S(x) \\ S(x)^{T} & R(x) \end{bmatrix} > 0 \tag{2.3}$$

Work of [52], as well as other published papers, present proof of Schur complement. Authors of [50], have notably proposed a formal theoretical strategy for robust MPC formulation through an online robust MPC algorithm using LMI principles and concepts. The LMI algorithm apart from being able to comply with set process constraints can guarantee robust stability. The LMI concept is used in chapter 4 of this research. [53]. The speed of this algorithm for online computations is very high and that satisfies one of the solutions to the DMPC limitation for LFC in power systems.

2.3 Explicit linear model predictive control

The major goal of all MPC algorithm development is to reduce online computational burdens to aid in online processes and this is key importance for real-time implementation for LFC in power systems and the computational burden is a major drawback and is computationally expensive when considering constraints in optimization problem solutions and the requirements grow exponentially with an increase in interconnected power systems. To reduce computation timing, LMI was used with convex optimization and with an observer system to run model state estimation simultaneously so that the system can then track in real-time. From RDMPC formulation, LMI with the explicit feedback formulation and objective function solution helps in the fast state data processing.

Some authors like in [54], develop an offline MPC framework comprising of three main steps they are; by using a multi-parametric programming approach to find a solution to the optimization problem offline, carry out state-space partitioning and finding online optimal control moves. A significant number of researchers have presented on the development of multi-parametric or explicit MPC algorithms.

Authors in [55], developed a strategy for explicit linear MPC based on a multi-parametric programming approach. A solution of state feedback that they arrived at was for nominal MPC.

A drawback is that a perfect model was assumed, and the model uncertainty was not considered. From a general standpoint, all the explicit MPC strategies have an inadequacy of the unique problems of complexity due to the computational burden that grows with the objective problem magnitude [54,56]. Research works are still ongoing to overcome this problem.

2.4 Adaptive model predictive control (AMPC)

Research into robust DMPC by authors [57,58], shows the promising advantages of the RDMPC with other MPC control methodologies. Despite the obvious advantage they may have, most MPC still suffer from some system varying dynamics and uncertainties. This is to note that since the development and analysis of MPC and RDMPC algorithms, assumptions are always made that

the internal plant state matrices were constant just like the traditional MPC despite its robustness. In the design of MPC controllers, the assumption is often made about state variable information available at the start. The assumption is that all the state variables are measurable and available. Not all state variables are available, even when available are not measurable or some are even impossible to measure. This constant state model assumption at most MPC algorithm development has already caused a design flaw in the practicality of that algorithm as such assumptions make MPC poor in handling plant varying dynamics which constantly changes operating conditions for every time step. The solution to this inadequacy, an adaptive MPC controller is developed in chapter 5, that have dynamic characteristics that change with the system plant changing dynamics and uncertainties that will help to effectively track the changing operating points, and used as an improvement over RDMPC that is capable of providing linear plant model update for each time step based on change in operating conditions during prediction horizon duration therefore providing more accurate predictions for the new and emerging operating conditions and be able to carry out its function in polynomial time and applicability for online application [59,60].

The approach adopted in this research to achieve an adaptive MPC algorithm is to use the state variables that correspond to the input and output using expanded state-space modelling in line with using an estimation system to obtain the state variable from the process measurement and developed an observer system using a mathematical model of the actual plant, this will help in state estimation, disturbance modelling for the systems.

2.5 Observer system modelling for distributed MPC

The impracticality of measuring all interactive states of a large system cannot lead to a method of estimating some of these interactive states of the subsystem are available through measurement and computation data and this has been identified as a key component in practical MPC implementation. Kalman filter is commonly used for a centralized system and it needs measurement data from all subsystems for accurate state estimation. Ce-MPC linear estimation theory is already well established but for large geographical interconnected systems, constraints makes it impossible to use centralized estimation methods added to the fact of considering issues of data redundancy and robustness, for such large networked systems it would require larger measurements data, difficulty in inter-communication of such large data of each subsystem let alone the problem of such voluminous data communication to a central processor for execution of estimation algorithms [61]. To handle the difficulty in centralized processing of large data, parallel solution techniques for estimation were designed [61]. Even when it seems that the problem is taken care of, there is still the part the central processors must update overall system error covariance for each time step. Theoretically, every stage in a centralized control system

serves as a benchmark for other system structures. For example, the centralized estimator serves as a benchmark for which the different distributed estimation strategies are compared. In [62-64], a state estimator framework for decentralized large-scale systems was designed. In this framework, the local estimators were designed considering decentralized dynamics and to account for other subsystem interactions, compensatory inputs were added. The implication is that the estimator convergence is based on the assumptions on how strong interconnections are on the interconnection matrix structure.

One method for removing steady-state offset, constant system disturbances (internal or external) and plant-model mismatch is disturbance modelling and the most used method is output disturbance modelling to help achieve good control performance without zero offsets at steady state [65,66]. Another option for this approach is using input disturbance models. In this model approach the disturbances entry point is assumed at the inputs instead, then derivative conditions are sort out in bearing with un-modelled effects, nonzero mean disturbances to guarantee to zero offset control, using suitable input disturbance models.

There are several disturbance model choices to choose from when considering the DMPC framework. One main goal of using the input disturbance model and estimator for the system is to help in effectively tracking nonzero output set points using required input state targets that can pull the system towards expected steady-state output conditions/targets. In [67,68], it was pointed out that distributed MPC framework optimal steady-state targets can be determined by performing a centralized target computation [69,70], or uses the alternative of computing the target by formulating it in a distributed approach with each subsystem computing their targets locally.

CHAPTER 3

MODELLING OF POWER SYSTEM

3.0 Methodology overview for LFC

LFC is a control scheme used to balance generated power with load demand including the power flows between area tie-lines in an interconnected power plant. LFC's major control purpose is keeping system frequency at the accepted required nominal value, by keeping the tie-line power flows and area control error at their required values. For optimal quality of power, the frequency is normally 60Hz or 50Hz as used in different parts of the world. When there is a deviation in this required frequency, the LFC schemes return the frequency to required value to maintain the quality of power supply and to prevent total breakdown of power plant [72]. Figure 3-1 presents a block diagram representation of synchronous generators with a frequency control loop. From the block diagram, Δf is frequency deviation, ΔP_L is the load disturbance, ΔP_c is speed changer motor output, ΔP_g is the speed governor output and ΔP_m is the turbine output power.

It is assumed that there is a load disturbance, the generated power is adjusted subsequently to balance the changes in load. The turbine mechanical output power is varied accordingly to the generation power, which in turn varies the speed governor output. Power system LFC control issues make primary frequency control inadequate hence additional frequency controller is used to alter the load reference point through the speed changer motor, the generator must be continually regulated to match the load disturbance to satisfactory keeps the frequency at near-constant. The control of frequency and the output power is called the LFC scheme, the controller used for LFC could be PI, PID, MPC or other advance controllers [2,72]. In the next sub-section, the MPC control structure is discussed and its application to the power system to improve the optimization process.

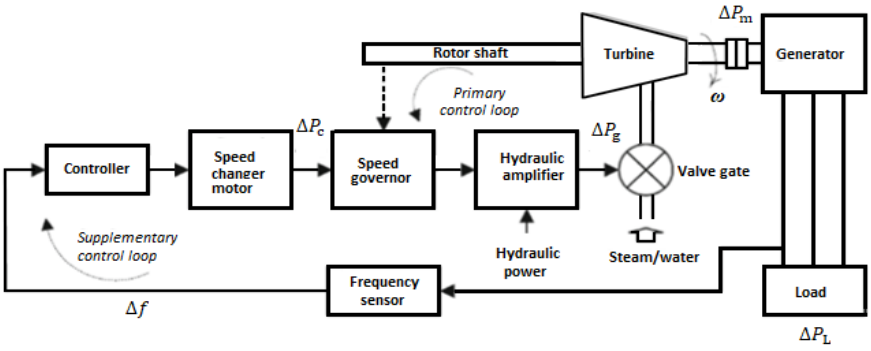

Figure 3-1 Block diagram of a synchronous generator with basic frequency control loops [73].

3.1 MPC control structure

In the literature [73], attention was focused on a single power plant in a network. This was at the initial state of LFC research. The promising results of the research led to multi-plant and multi-agent networked control systems. Similarly, modelling and control have increased the drive to exploit different control algorithms to take care of different LFC problems. This dissertation also focuses on the review of robust MPC control structures and architectures for large scale IPS [74]. In MPC control systems, the controllers apply MPC feedback policies to their local subsystems. Based on the topology they might communicate their predictions between themselves (subsystems) and therefore integrate the information obtained into their local MPC objective problem, which leads to better coordination within the subsystems in the full network [75].

A large power system network usually comprises different physically or geographically separated subsystems. The end goal for the subsystem controllers is to arrive at a common global performance of this entire system. Centralized MPC structure naturally imposes high computational complexity in communication bandwidth, hence the difficulty in its control led to the development of several distributed MPCs structure [76]. MPC has enjoyed the successful application in handling optimization processes in other to compute optimal control moves in a power system LFC within the realistic power system constraints [30]. Figure 3-2 shows the basic description of MPC block diagram, where u is the actuator, $\emptyset$ and τ are the constant matrices, r is the input variable and y is the predicted output variable.

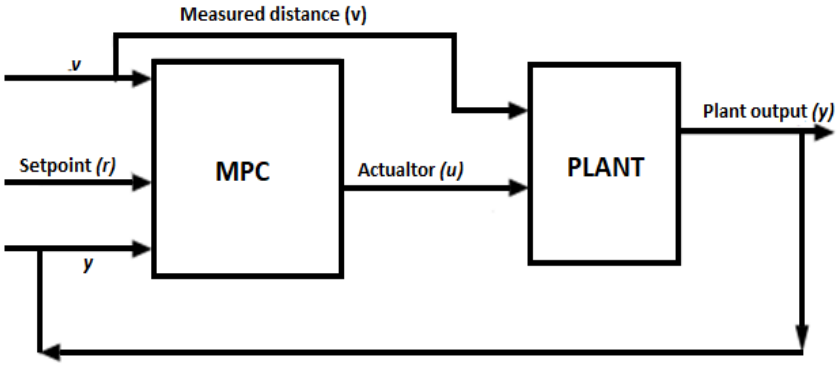

Figure 3-2 Block model of model predictive control [30].

3.2 Interconnected power system

The power system may consist of several CA that are interconnected by tie-lines as illustrated in Figure 3-3. The control goal here is keeping the net active power flow between the interconnected

areas within a set limit. The interconnected power system normally consists of a minimum of two CA. Power subsystems can have a thermal system, hydropower systems, renewable or nuclear power-based systems. However hydro and thermal power systems were considered in this dissertation as they are most involved in load frequency control.

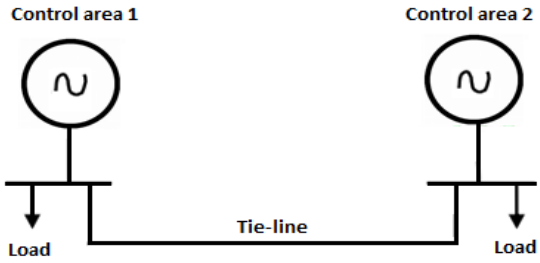

Figure 3-3 Two area interconnected power system [80].

3.3 Model of power plant components

Figure 3-4 presents a typical conventional single-area power plant. The major components hydraulic amplifier, speed governor, speed changer and control valve with a linkage mechanism connecting them, as in [78]. A linkage mechanism from Figure 3-3 has *A*, *B*, and *C* while *C*, *D*, and *E* are in another unit. The steady-state output power of the turbine is denoted as ΔP_c. When in operation *A* and *B* moves downward; *C* and *D* move upwards while *E* moves downwards. This movement pattern allows increased steam volume into the turbine which results in generated output power increase. The pilot valve is controlled by high-pressure oil. The main piston is made up and downwards depending on the *E* position. ΔP_g, is the speed governor output and corresponds to ΔX_C movement as presented in Figure 3-3. The reference input ΔP_c and frequency deviation Δf are two inputs to speed governor. These $\Delta X_A, \Delta X_B, \Delta X_C, \Delta X_D, \Delta X_E$ parameters are the links displacement of *A* , *B* , *C* , *D* , *E* . Their movements are in millimetres, but then it is normally defined in per unit megawatts (p.u MW).

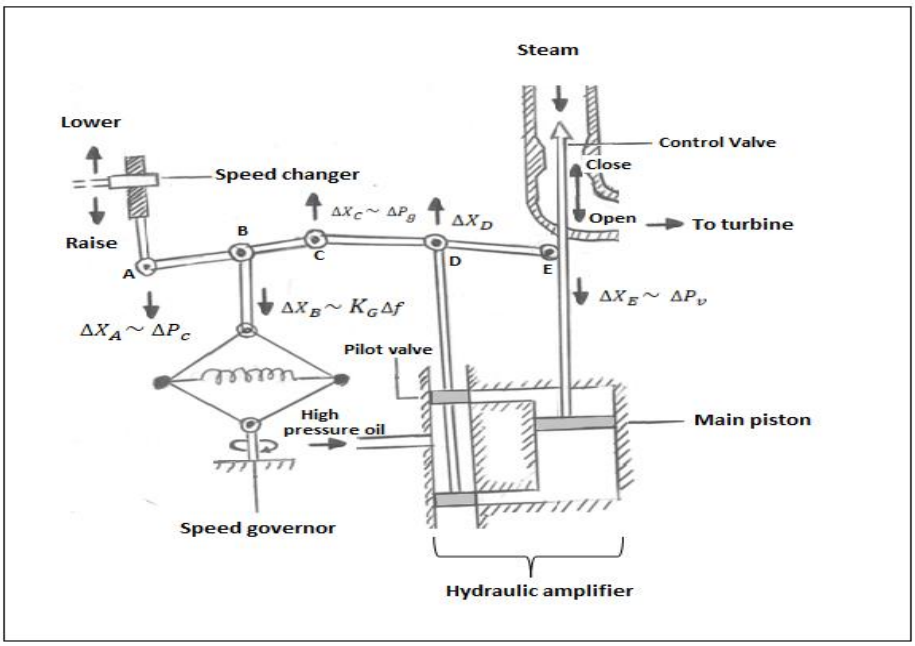

Figure 3-4 Diagram of a typical single area power system [80].

3.3.1 Governor

Based on the operation of the conventional single area power system in Figure 3-4, a positive change in ΔP_c will lead to a positive change in ΔP_g likewise a positive change in Δf will result in a downward movement of linkage B and C as in [78], leading to negative ΔP_g, thus

$$\Delta P_g = \Delta P_c - \frac{1}{R}\Delta f \tag{3.1}$$

R denotes the speed regulation of the governor in Hz /MW.

In [79], the Laplace transform (LT) of (3.1) is given as

$$\Delta P_g(s) = \Delta P_c(s) - \frac{1}{R}\Delta f(s) \tag{3.2}$$

Figure 3-5 shows the block diagram of equation (3.2) similar in [79]. The hydraulic actuator output is ΔP_v, while ΔP_g and ΔP_v are inputs to ΔX_D. A positive change in ΔP_g, means a change in ΔX_D is also positive and ΔP_v negative change implies a positive change in ΔX_D. Thus

$$\Delta X_D = \Delta P_g - \Delta P_v \tag{3.3}$$

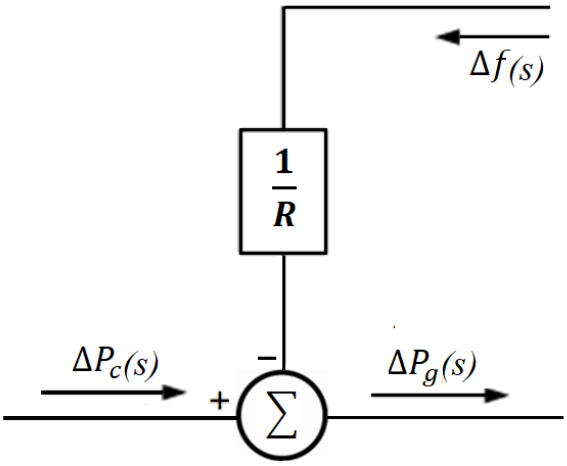

Figure 3-5 Block diagram of speed governor [80].

Then hydraulic actuator input and output relationship in [79], is represented by

$$\Delta P_v = K_G \int \Delta X_D dt \tag{3.4}$$

Performing LT on (3.3) and (3.4) leads to (3.5) and (3.6) as show in [79], as follows:

$$\Delta X_D(s) = \Delta P_g(s) - \Delta P_v(s) \tag{3.5}$$

$$\Delta P_v(s) = \frac{KG}{S} \Delta X_D(s) \tag{3.6}$$

Substituting (3.5) into (3.6) and eliminating the $\Delta X_D(s)$, the relationship between ΔP_v(s) and $\Delta P_g(s)$ is given as

$$\Delta P_v(s) = \frac{1}{1+sT_G} \Delta P_g(s) \tag{3.7}$$

where T_G is governor time constant expressed as

$$T_G = \frac{1}{K_G} \tag{3.8}$$

Rewriting (3.7) as (3.9), T_G represents the governor time constant that is around 0.1s for power system having a reheat turbine

$$G_H(s) = \frac{\Delta P_v(s)}{\Delta P_v(s)} = \frac{1}{1+sT_G} \tag{3.9}$$

The speed governor and hydraulic actuator block diagram of Figure 3-6 is obtained by combining (3.2) and (3.9),

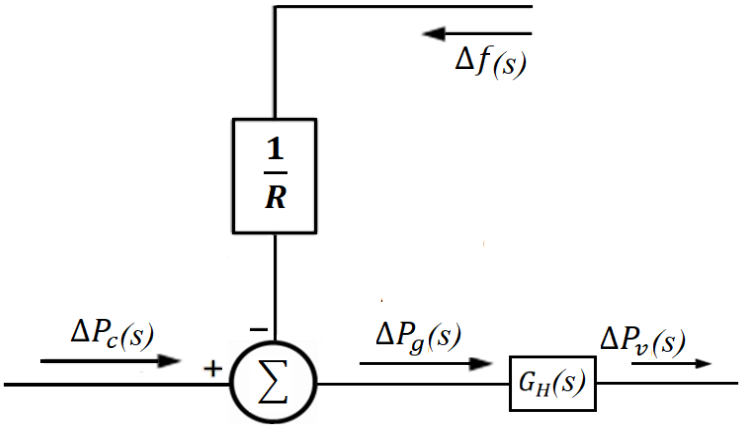

Figure 3-6 Speed governor block diagram with a hydraulic valve actuator [80]

The speed governor has nonlinear behaviour, which includes GDB [80, 81, 82, 83]. This means that the speed governor does not change speed immediately when there is a change in the input signal. It only changes when the input signal attains a specified value. GDB is a limitation in all power plant governors when the set limit is exceeded [84].

3.3.2 Turbine

Normally, the turbine output power P_m is balanced with generation output power P_g, to give constant speed and frequency leading to zero accelerations [79]. ΔP_m represents turbine power change while ΔP_g generator output power change. Keeping frequency deviation Δf at zero [79], the power acceleration, ΔP_A [78], is given as

$$\Delta P_A = \Delta P_m - \Delta P_g \tag{3.10}$$

In (3.10), it clearly shows that a positive ΔP_A or $\Delta P_A > 0$ will lead to acceleration and deceleration if $\Delta P_A < 0$. The design of a reheat turbine often for large units similar to what is shown in Figure 3-7, having two stages of high pressure (HP) and low pressure (LP) increases efficiency [78].

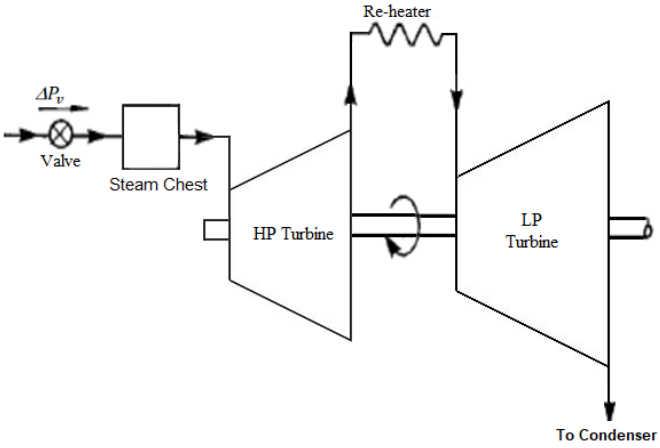

Figure 3-7 Reheat turbine [85].

Furthermore, the penstock in hydro turbines builds up the water pressure in it by changing the vertical drop as water flows through it from the "head". The non-reheat turbine transfer function *GT(s)* expression is in (3.11), where T_T is the turbine time constant. Typically, 100ms $\leq T_T \geq$ 500 ms [79]

$$G_T(s) = \frac{1}{1+sT_T} \tag{3.11}$$

The high pressure of the reheat turbine as in [78], adds to the power component as shown in (3.12)

$$\Delta P_{THP}(s) = \frac{K_r}{1+s\,T_T}\,\Delta P_v(s) \tag{3.12}$$

where $\Delta P_{THP}(s)$ is the high-pressure transfer function part of the reheat turbine with K_r as the high-pressure rating. The LP turbine as in [78], adds to the power component of (3.13).

$$\Delta P_{TLP}(s) = \frac{1-K_r}{(1+s\,T_T)(1+sT_{RH})}\,\Delta P_v(s) \tag{3.13}$$

where $\Delta P_{TLP}(s)$ is low-pressure stage transfer function of reheat turbine, T_{RH} is the time delay between the HP stage and LP stage, and $4 \leq T_T \geq 10$ (sec). The output of the reheat turbine as in [78], is the sum of the outputs of HP and LP stages as shown in (3.14), where $G_{TRH}(s)$ is reheat turbine transfer function

$$G_{TRH}(s) = \frac{1-sK_rT_{RH}}{(1+s\,T_T)(1+sT_{RH})}$$

(3.14)

K_r is the re-heater gain and specified as

K_r = 1- a fraction of steam reheated and in cases of no reheat, K_r=1.

T_w from the transfer function expression of (3.15), is the water starting time there is a delay for the water to get heated up this is given as, which is given as S = $\frac{1}{T_w}$, then

$$G_T(s) = \frac{1-sT_w}{1+0.5sT_w} \tag{3.15}$$

In (3.16), it shows the function of the hydro turbine transient response coefficient, with T_R as reset time, temporary droop coefficient as ΔR_T and permanent droop coefficient *as* ΔR_P, and

$T_2 = (R_T T_R) / R_P$.

$$G_{TRH} = \frac{1+T_R s}{\left(1+\left(\frac{T_R}{R_P}\right)s\, T_R\right)} = \frac{1+T_R s}{(1+T_2 s)} \tag{3.16}$$

All generating plants have a rate of change limits of power generated in [71], either maximum or minimum, hence the inclusion of GRC in turbine systems, Figure 3-8 shows the nonlinear turbine model with GRC and they have typical values of 10% p.u/min for reheats turbine system and a dead band of $\pm$0.036Hz as in [85,86].

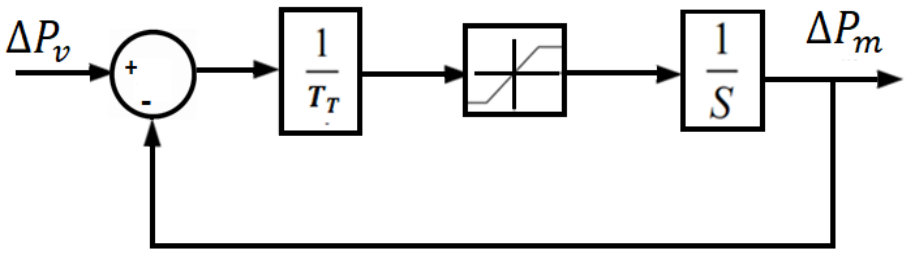

Figure 3-8 Generation rate constraint in nonlinear turbine model [80].

3.3.3 Generator

The frequency of the power generated by a power system that is balanced is normally 60Hz or 50Hz as used in different parts of the world. The expression K^0_{kin} MW sec represents the kinetic energy of the rotating body. When a load is increased (ΔP_L), generated power increases by ΔP_g in order to balance the load increase depicted in (3.3) [78]. There is always some time delay before the control valve will act to increase the turbine power. It is a point of note that turbine power is not always equal to the generated power resulting in the power imbalance that is denoted as $\Delta P_m - \Delta P_g$ resulting in undue speed/frequency changes [78]. Kinetic energy attained is

proportional to the square of the speed where f^0 the normal frequency from (3.17) and f is the actual frequency with K^0_{kin} is rated kinetic energy [79].

$$K_{kin} = K^0_{kin}\left(\frac{f}{f0}\right)^2 MW\,s.\,K \tag{3.17}$$

In (3.18) it shows load demand change over frequency change where D_k denotes demanding coefficient similar to [78],

$$D_k = \frac{\partial P_L}{\partial f} MW\,Hz. \tag{3.18}$$

Resulting to:

$$\Delta P_m - \Delta P_L = \frac{d}{dt}(K_{kin}) + D_k \Delta f \tag{3.19}$$

where frequency deviation Δf and $f = f^0 + \Delta f$. From (3.17), we derive K_{kin} derive in [78], as

$$K_{kin} = K^0_{kin}\left[\left(\frac{f^0 + \Delta f}{f^0}\right)^2 = K^0_{kin}\left[1 + \frac{2f^0\Delta f}{f^0} + \left(\frac{\Delta f}{f^0}\right)^2\right] \approx K^0_{kin}\left(1 + \frac{2f^0\Delta f}{f^0}\right) MW\,s \tag{3.20}$$

The derivative of K_{kin}

$$\frac{d}{dt}(K_{kin}) = \frac{2K^0_{kin}}{f^0}\frac{d}{dt}\Delta f \tag{3.21}$$

Substituting (3.21) into (3.20), hence (3.22) becomes

$$\Delta P_m - \Delta P_L = \frac{2K^0_{kin}}{f^0}\frac{d}{dt}\Delta f + D_k \Delta f \tag{3.22}$$

From (3.23) H is per unit inertial constant and P_r as generator power rating.

$$H = \frac{K^0_{kin}}{P_r}\ s \tag{3.23}$$

plugging (3.23) into (3.22), the expression similar [78], becomes.

$$\Delta P_m - \Delta P_L = \frac{2HP_r}{f^0}\frac{d}{dt}\Delta f + D_k \Delta f \quad puMW \tag{3.24}$$

Laplace transform of (3.24) becomes

$$\Delta P_m(s) - \Delta P_L(s) = \frac{2HP_r}{f^0}(s)(\Delta f(s) + D_k \Delta f(s) \tag{3.25}$$

$\Delta f(s)$ is derived from (3.25) as in [78],

$$\Delta f(s) = \frac{I}{\frac{2HP_r}{f^0}(s) + D_k}[P_m(s - \Delta P_L(s)] \tag{3.26}$$

This can be re-written as,

$$\Delta f(s) = G_P(s)\,[\Delta P_m(s) - \Delta P_L(s)] \tag{3.27}$$

$G_P(s)$ in (3.27), is given as

$$G_p(s)\,\frac{\frac{1}{2HPr}}{f^0}s + D_k = 1 + \frac{\frac{1/D_k}{2HPr}}{Lf^0}s = \frac{K_p}{1+sT_p} \tag{3.28}$$

where $K_p = \frac{1}{D_k}$, and $T_r\,\frac{2H_r}{D_k f^0}$

The closed-loop is shown in Figure 3-9 combining (3.28) to the system.

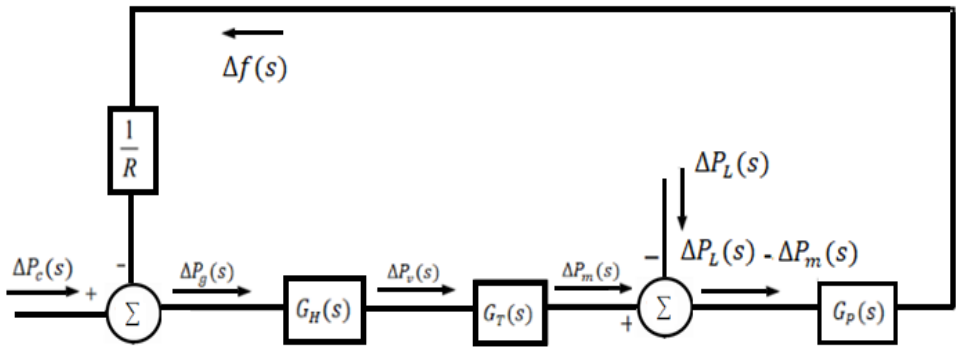

Figure 3-9 Block diagram illustration of close loop primary LFC [78].

The speed adjuster must operate as frequency changes to keep frequency error at zero. Integral control is introduced at this point to amplify and integrate frequency error. Negative frequency error will affect control command to cause the signal ΔP_c to go negative as in (3.29) and K_1 is controller gain constant [79]

$$\Delta P_c = -K_1 = \int \Delta f dt \tag{3.29}$$

Laplace transform of (3.39) is given as

$$\Delta P_c = -\frac{K_1}{s}\Delta f(s) \tag{3.30}$$

The integrator accepts frequency error Δf as input and its output control the speed changer. A complete LFC block diagram complete LFC equipped with an integral controller shown in Figure 3-10. It is also important to put into consideration that for conventional control the integral controller was used but due to its inadequacies the MPC controller is being used to replace it. For this reason, the final power system diagram will be replaced by the MPC block.

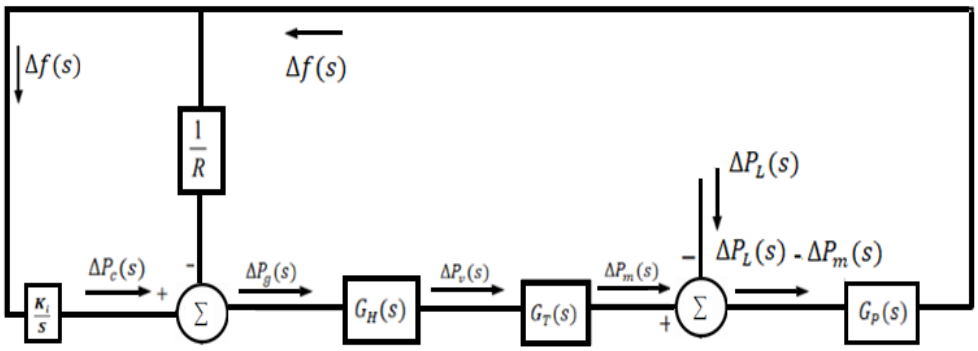

Figure 3-10 Complete LFC equipped with an integral controller [79].

A non-zero in frequency error, will result in an increase in integral controller output and alter speed adjuster excursions as integral controller output is directly connected to the speed changer. The output of the integrator controller will be at zero if the frequency error is kept at zero making speed changer to remain at a constant position/value [79].

3.3.4 Tie-line power deviation

Tie-line active power deviation flow referred to as static error which implies that an area must support other areas to achieve steady-state. The active power flow between *i* and *j* during nominal conditions as in [79], is expressed as

$$P_{tie,ij} = \frac{[V_i][V_j]}{X} sin(\delta_i^0 - \delta_j^0) \tag{3.31}$$

V_i and V_j are the voltages in area *i* and *j* respectively with δ_i^0, δ_j^0 as the angles of the voltages in area *i* and *j* respectively. $\Delta P_{tie,ij}$ an expression for a small change in the angles δ_i^0 and δ_j^0 is given as [78]

$$\Delta P_{tie,ij} = \frac{[V_i][V_j]}{X} \cos(\delta_i^0 - \delta_j^0)(\delta_i - \delta_j) \tag{3.32}$$

Frequency *f* and angular frequency ω are related by the expression of (3.33), where δ_s is the angle.

$$f = \frac{w}{2\pi} = \frac{1}{2\pi}\frac{d\delta_s}{dt} \tag{3.33}$$

$$\delta s = 2\pi \int_0^t f dt \tag{3.34}$$

Similar in [80], Δf_1 and Δf_2, and $\Delta P_{tie,ij}$ are given as

$$\Delta P_{tie,ij} = 2\pi(\int_0^t \Delta f_i dt - \int_0^t \Delta f_j dt) \tag{3.35}$$

In (3.35) Laplace transform is expressed as

$$\Delta P_{tie,ij} = \frac{2\pi}{S}[\Delta f_i(s) - \Delta f_j(s)] \tag{3.36}$$

it can be represented by the block diagram presented in Figure 3-11.

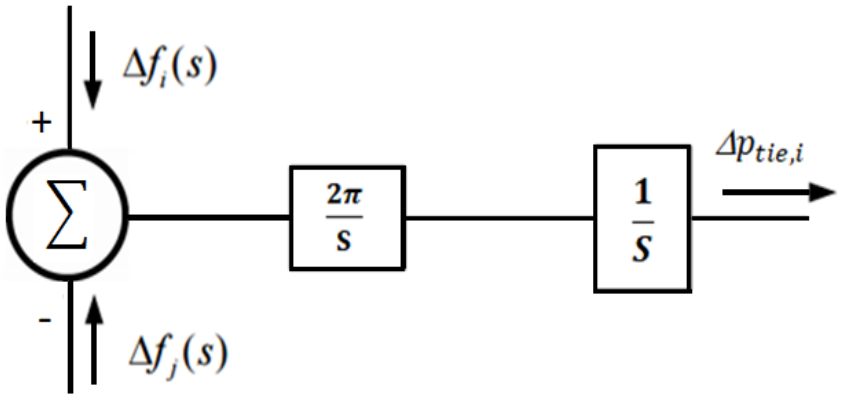

Figure 3-11 Block diagram representation of tie-line power deviation [79].

3.3.5 Area control error

LFC scheme is used continually to keep frequency at 50/60Hz within the allowable permissible limit of $\pm$0.5Hz such that tie-line errors tend toward zero while maintaining the scheduled power interchange in the power system. ACE is introduced to help the system meet the set objectives [87 – 89]. In [86], ACE indicates power variation between the generation and the load, ACE_i is deduced as the summation of the frequency deviation (Δf_i) multiply by a bias factor (B_i) and the tie-line active power deviation ($\Delta P_{tie,ij}$).

$$ACE_i = \sum_{j=1,2.....N, j\neq i} \Delta P_{tie,ij} + B_i \Delta f_i \tag{3.37}$$

The implication of (3.37) is that for ACE to be zero, both frequency and tie-line power change errors must be at zero thus all control structure goals is always to force ACE to zero.

3.4 Hydro and thermal power plant

The block diagram in Figure 3-12 presents the control area for a thermal power plant, GRC is presented in Figure 3-13 similar to [71, 72, 77-80]. The block diagram of a hydropower plant is shown in Figure 3-14 with GRC in Figure 3-15, all having the proposed MPC block replacing the traditional integral controller.

From the block diagrams in Figure 3-12 to 3-15, area i, =(1,2,3), load disturbance is ΔP_L, frequency deviation is Δf_i and ΔP_{tie} is tie-line active power deviation, area control error is ACE_i, the control input signal is u_i, the frequency bias factor is B_i, R_i is the speed due to governor action of area i, generator power deviation is ΔP_m , governor valve position valve servomotor position is ΔP_v and ΔP_{gi} respectively and rotor angular distance is $\Delta\delta$, Power system time out is T_P, reheat turbine gain is K_{ri}, reheat time constant is T_r, the governor time constant is represented as T_{Gi} , T_R is reset time, and T_W is the water starting time [78].

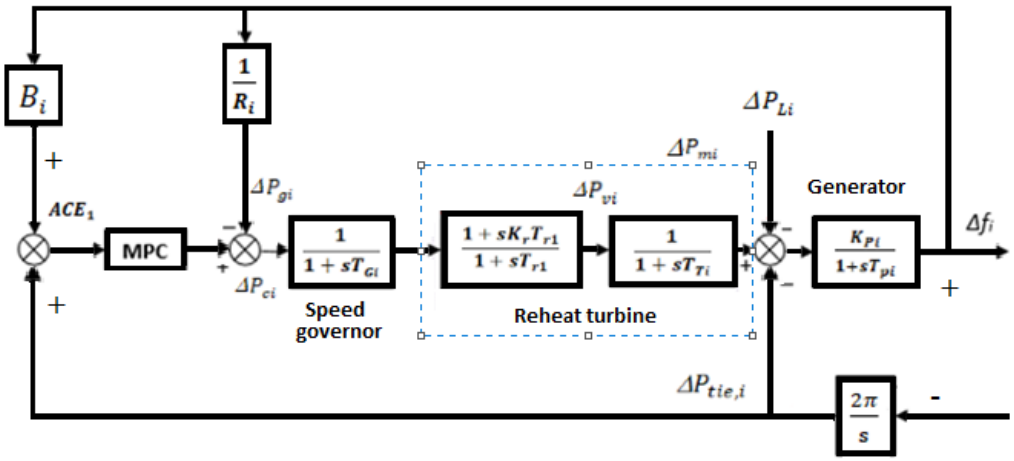

Figure 3-12 Block diagram representation of the control area *i* thermal plant [71,78]

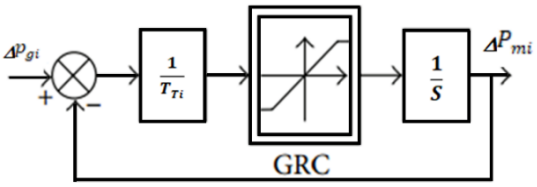

Figure 3-13 GRC in thermal power system [71,78]

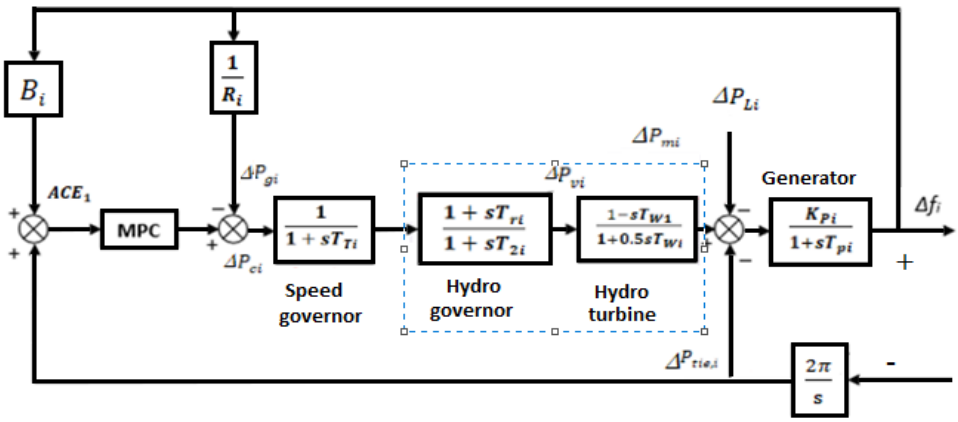

Figure 3-14 Block diagram representation of the control area *i* hydropower plant [71,78]

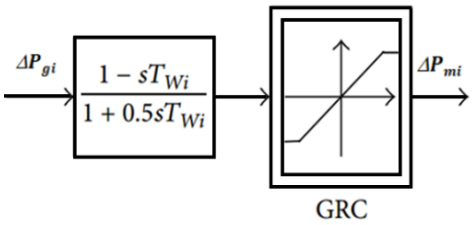

Figure 3-15 GRC in the hydropower system [71,78].

CHAPTER 4

ROBUST DISTRIBUTED MPC

4.0 Robust DMPC for load frequency control

LFC functions to continually balance the frequency at the schedule value of power system and continually keeps ACE tending towards zero. This is achieved by regulating the generator units to adjust active power to regulate power generation with load power demand to keep their balance for the entire power system. Changes in system parameters and other non-linear factors significantly affect the dynamic response of power systems and tend to lead to bigger overshoot with a longer settling time which leads to power system instability [90]. Similarly, other factors affecting LFC performance include disturbances due to increased power system complexity, power system modelling errors and recently adopted changes in IPS structures. Any proposed solutions must consider the robustness of the LFC design method to ensure a reliable power supply.

MPC algorithm is well known in literature after the traditional PID controller for LFC control. It has been an attractive methodology for LFC, which also has the capability to achieve optimization procedures that can determine optimal control moves within realistic power system constraints over a future horizon. GRC is one of such constraint in LFC research. PID controllers and conventional MPCs as shown from researches are unable to explicitly absorb plant uncertainties, due to the modern power system increase in size and complexity. Thus, robust MPC was developed to handle plant uncertainties and have been recently improved upon to cater for power system parameter changes [91,92]. In some existing and conventional MPCs formulations, it is often presumed that all subsystems are identical, which in real power systems is not the case. Subsequently, several MPC controllers were developed such as distributed MPC, decentralized MPC, and centralized MPC to eliminate the above limitation [93, 94].

In this section, RDMPC scheme is developed for a two-area and three-area hydro-thermal power systems. The entire interconnected power system comprises of several subsystems, each subsystem objective function is formulated as a convex optimization problem with linear matrix inequalities (LMI) for an effective solution using the RDMPC algorithm. This proposed method exhibits robustness when compared with conventional PID in the presence of parameter change and nonlinear constraints [90].

The remaining sections of this chapter are presented as; Section 4.1, presents the mathematical model of the power system proposed. Section 4.2, shows the RDMPC algorithm as discussed in this section with the LMI constraints. Section 4.3, simulation result and analysis 4.4, conclusion.

4.1 Power System model

A block diagram of two-area and three-area hydro-thermal interconnected power plant is presented in Figures 4-1 and 4-2 respectively, it is shown that each area has its own MPC controller and each CA is linked through their tie-lines. The interconnection consequence is that any sudden load disturbance in any CA all other interconnected CA's are affected. MPC controllers act accordingly and go into action to normalize the frequency to its original required value, by keeping the tie-line and ACE towards zero [90,91,96-97]. To develop the RDMP for the LFC, the system has to be *linearized* using the power system parameters. The parameter used for the hydro and thermal plant are given in Table A-1 (Appendix A).

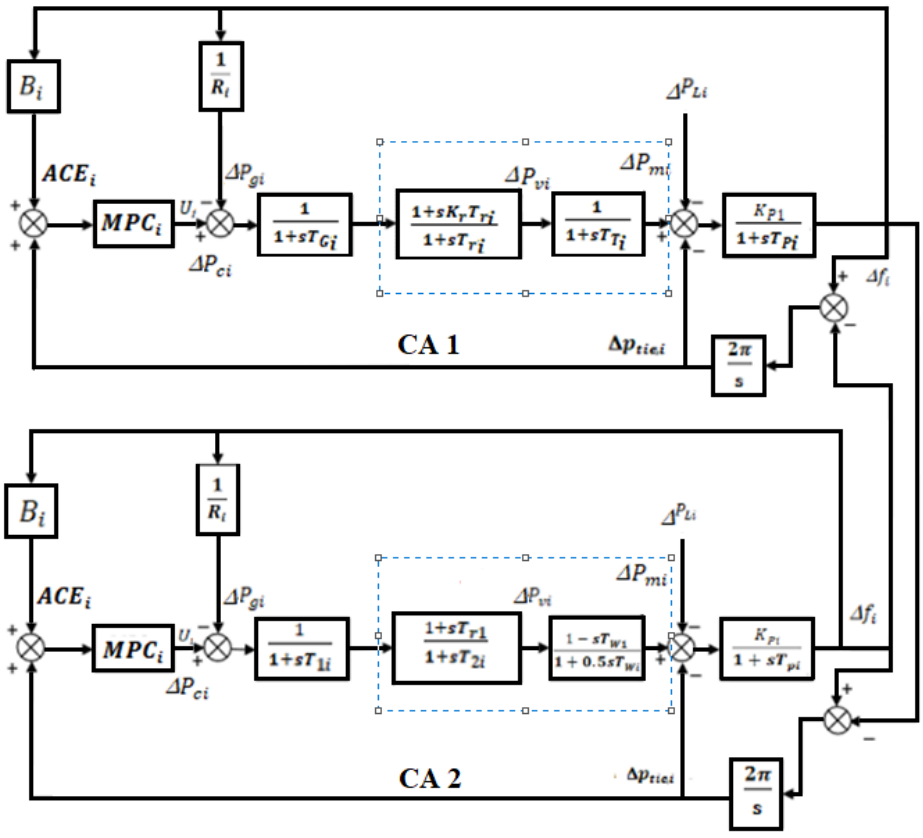

Figure 4-1 Block diagram representation of a two-area hydro-thermal power system [59]

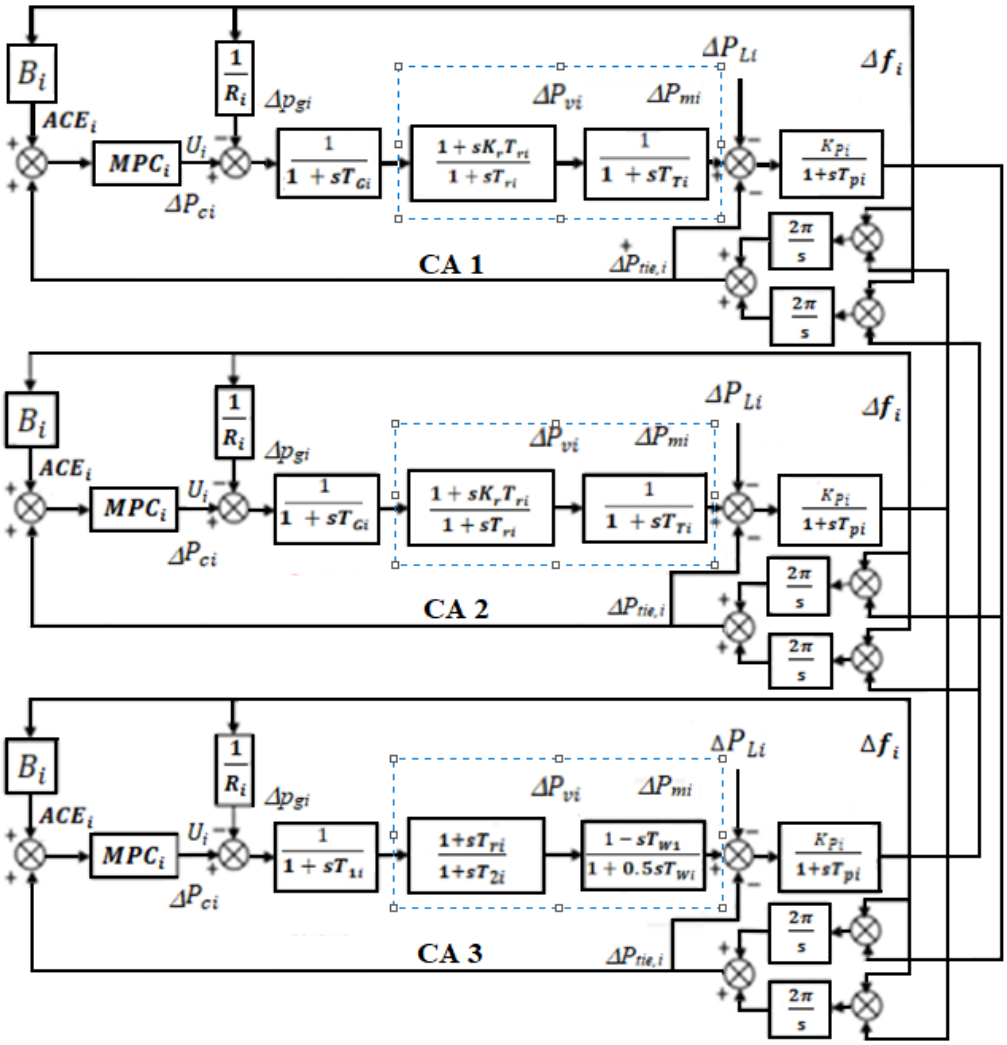

Figure 4-2 Block diagram representation of a three-area hydro-thermal power system [59]

4.1.1 Thermal power system model

In [94], the thermal plant has a speed governor subsystem (SG), reheat time delay RTD, steam turbine unit (STU) and power system (PS), using the block diagram from Figure 4-1 for the two-area hydro-thermal plant as a reference model. For any change in load, frequency deviation Δf_i are computed as follows [99]

$$\Delta \dot{f}_i = -\frac{1}{T_{pi}}\Delta f_i - \frac{K_{pi}}{T_{pi}}\Delta P_{tie,i} + \frac{K_{pi}}{T_{pi}}\Delta P_{mi} - \frac{K_{pi}}{T_{pi}}\Delta P_{Li} + \frac{1}{T_{Gi}}\Delta P_{ci} \tag{4.1}$$

The dynamic of the system can be express as

$$\Delta \dot{P}_{gi} = -\frac{1}{T_{Ti}}\Delta P_{gi} = -\frac{1}{T_{Ti}}\Delta P_{vi} \tag{4.2}$$

The dynamics of the governor can be expressed as

$$\Delta\dot{P}_{mi}=\frac{1}{T_{Gi}R_i}\Delta f_1-\frac{1}{T_{Gi}}\Delta P_{mi} \tag{4.3}$$

Turbine dynamic equation (reheat) is given as

$$\Delta\dot{P}_{vi}=\frac{1}{T_{Gi}R_i}\Delta f_i+\left(\frac{1}{T_{ri}}-\frac{K_{ri}}{T_{Gi}}\right)\Delta P_{gi}-\frac{1}{T_{ri}}\Delta P_{vi} \tag{4.4}$$

Area *i* and *j* tie-line power exchange is described as

$$\Delta\dot{p}_{tie}^{ij}=-K_{sij}(\Delta f_i-\Delta f_j),\Delta P_{tie}=-\Delta p_{tie}^{ij}. \tag{4.5}$$

The total tie line change between area *i* and *j* and other areas can be computed as

$$\Delta\dot{P}_{tie,i}=\sum_{\substack{j=1\\ j\neq i}}^{N}\Delta p_{tie}^{ij}=\sum_{\substack{j=1\\ j\neq i}}^{N}K_{sij}(\Delta f_i-\Delta f_j) \tag{4.6}$$

The ACE indicates a discrepancy between power, area load, and generation.

$$ACE_i=[B_i\Delta f_i+\Delta P_{tie,i}] \tag{4.7}$$

In [99], frequency response model (4.1) to (4.4) and (4.6), combine, let assume *N* is representing a number of CA of the power system as used in (4.6), for area-*i*, the state-space model is given as:

$$\cdot\begin{bmatrix}\Delta\dot{f}_i\\ \Delta\dot{P}gi\\ \Delta\dot{P}mi\\ \Delta\dot{P}vi\\ \Delta\dot{P}tie,i\end{bmatrix}=\begin{bmatrix}-\frac{1}{T_{pi}} & -\frac{K_{pi}}{T_{pi}} & \frac{K_{pi}}{T,P} & 0 & 0\\ 0 & 0 & -\frac{1}{T_{Ti}} & 0 & \frac{1}{T_{Ti}}\\ -\frac{1}{T_{Gi}R_i} & 0 & 0 & -\frac{1}{T_{Gi}} & 0\\ -\frac{K_{ri}}{R_iT_{Gi}} & 0 & 0 & \frac{1}{T_{ri}}-\frac{K_{ri}}{T_{Gi}} & \frac{1}{T_{ri}}\\ \sum_{j\neq 1}T_{sij} & 0 & 0 & 0 & 0\end{bmatrix}\begin{bmatrix}\Delta\dot{f}_i\\ \Delta\dot{P}gi\\ \Delta\dot{P}mi\\ \Delta\dot{P}vi\\ \Delta\dot{P}tie,i\end{bmatrix}$$

$$+\begin{bmatrix}0\\ 0\\ \frac{1}{T_{Gi}}\\ 0\\ 0\end{bmatrix}\Delta p_{ci}+\begin{bmatrix}-\frac{K_{pi}}{T_{pi}}\\ 0\\ 0\\ 0\\ 0\end{bmatrix}\Delta p_{ci}+\begin{bmatrix}0\\ -T_{12}\\ 0\\ 0\\ 0\end{bmatrix}\Delta p_{Li} \tag{4.8}$$

$$y=ACE_i[\mathrm{B_i}1\ 0\ 0\ 0]\begin{bmatrix}\Delta\dot{f}_i\\ \Delta\dot{P}gi\\ \Delta\dot{P}mi\\ \Delta\dot{P}vi\\ \Delta\dot{P}tie,i\end{bmatrix} \tag{4.9}$$

With a set of variable $x_i=[\Delta f_1\ \Delta P_{gi}\ \Delta P_{mi}\ \Delta P_{vi}\ \Delta P_{tie,i}]^T$ the state vector for thermal is given as

$$\boldsymbol{A}_i=\begin{bmatrix} -\frac{1}{T_{pi}} & -\frac{K_{pi}}{T_{pi}} & \frac{K_{pi}}{T,P} & 0 & 0 \\ 0 & 0 & -\frac{1}{T_{Ti}} & 0 & \frac{1}{T_{Ti}} \\ -\frac{1}{T_{Gi}R_i} & 0 & 0 & -\frac{1}{T_{Gi}} & 0 \\ -\frac{K_{ri}}{R_iT_{Gi}} & 0 & 0 & \frac{1}{T_{ri}}-\frac{K_{ri}}{T_{Gi}} & \frac{1}{T_{ri}} \\ \sum_{j\neq 1} T_{sij} & 0 & 0 & 0 & 0 \end{bmatrix},$$

$\boldsymbol{B}_i = [0\ 0\ 0\ 0\ -\frac{1}{T_{Gi}}]$, $\boldsymbol{C}_i\ [-\frac{K_{pi}}{T_{pi}}\ 0\ 0\ 0\ 0]$,

$\boldsymbol{D}_i=[B1000]$. (4.10)

4.1.2 Hydropower system model

Hydropower plant composed of the governor system (SG), hydraulics turbine system (ST) and water hammer dynamic subsystem (SH). Figure 4-2, present the state-space model which can be formulated as followings [94]

SG: $\Delta\dot{P}_{mi}=2\alpha\Delta f_i-\frac{1}{T_{wi}}\Delta P_{mi}+2k\Delta P_{gi}+2\beta\Delta X_{ghi}$ (4.11)

ST: $\Delta\dot{P}_{gi}=-\alpha\Delta f_i-\frac{2}{T_{2i}}\Delta f_i-\beta\Delta X_{ghi}$ (4.12)

SH: $\Delta\dot{X}_{ghi}=-\frac{1}{T_{1i}R_i}\Delta f_i-\frac{1}{T_{1i}}\Delta X_{ghi}$ (4.13)

where,

$$\alpha=\frac{T_{Ri}}{T_{1i}T_{2i}R_i},\ \beta=\frac{(T_{Ri}-T_{1i})}{T_{1i}-T_{2i}},\ \kappa=\frac{(T_{2i}+T_{wi})}{T_{2i}T_{wi}}$$

In [94], the state vector for the hydropower plant is expressed as,

$x_i=[\Delta f_1\ \Delta P_{gi}\ \Delta P_{mi}\ \Delta P_{vi}\ \Delta P_{tie,i}]^T$

$$\boldsymbol{A}_i=\begin{bmatrix} -\frac{1}{T_{pi}} & -\frac{K_{pi}}{T_{pi}} & \frac{K_{pi}}{T,P} & 0 & 0 \\ -\alpha & 0 & 0 & \frac{1}{T_{2i}} & -\beta \\ 2\alpha & 0 & -\frac{2}{T_{wi}} & 2k & 2\beta \\ -\frac{1}{T_{1i}R_i} & 0 & 0 & 0 & -\frac{1}{T_{1i}} \\ \sum_{j\neq 1} T_{sij} & 0 & 0 & 0 & 0 \end{bmatrix},$$

$\boldsymbol{B}_i$= [0 0 0 $-2\mathrm{R_i}\alpha$ $-\frac{1}{T_{1i}}$], C_i [$\mathrm{B_i}$ 1 0 0 0],

$\boldsymbol{D}_i$= [$\mathrm{B_i}$ 1 0 0 0]. (4.14)

The interaction matrix between the control area are

$$\boldsymbol{A}_{ij}=\begin{bmatrix} 0 & 0 & 0 & 0 & 0 \\ 0 & 0 & 0 & 0 & 0 \\ 0 & 0 & 0 & 0 & 0 \\ 0 & 0 & 0 & 0 & 0 \\ T_{sij} & 0 & 0 & 0 & 0 \end{bmatrix}, \quad B_{ij}=[0\ 0\ 0\ 0\ 0]^T \tag{4.15}$$

An assumption adopted in this study is that the process model is a time-varying linearized mathematical model for thermal and hydropower plant and is in the form of [71];

$$\dot{\boldsymbol{x}}_i\,(t) = \boldsymbol{A}_{ii}\,(t)\,\boldsymbol{x}_i\,(t) + \sum_j \boldsymbol{A}ij \quad (t)\,\boldsymbol{x}_j\,(t) + \boldsymbol{B}_{ii}\,(t)\,u_i\,(t) + \boldsymbol{F}_{ii}\,(t)\,\boldsymbol{d}_i\,(t)\,, \tag{4.16}$$

where i represents the i^{th} control area;

$\boldsymbol{x}_i \in \mathbb{R}^{ni}$ represent the state, $\boldsymbol{u}_i \in \mathbb{R}^{mi}$ represent the input, $\boldsymbol{di} \in \mathbb{R}^{zi}$ represent the disturbance vector, in the *i-th* subsystem while $\boldsymbol{x}_j \in \mathbb{R}^{nj}$ is a state vector of the neighbour subsystem and output is

$$\boldsymbol{y}_i\,(t) = C_{ii}x_i\,(t) \tag{4.17}$$

Where $\boldsymbol{y}_i \in \mathbb{R}^{Vi}$ represents the output signal of the system. The matrices in (4.16) and (4.17) have the dimensions

$$\boldsymbol{A}_{ii} \in \mathbb{R}^{ni\ x\ ni}, \boldsymbol{A}_{ij} \in \mathbb{R}^{ni\ x\ nj}, \boldsymbol{B}_{ii} \in \mathbb{R}^{ni\ x\ mi}, \boldsymbol{F}_{ii} \in \mathbb{R}^{ni\ x\ zi}, \boldsymbol{C}_{ii} \in \mathbb{R}^{vi\ x\ ni}. \tag{4.18}$$

The state-space equation for the whole power system in [71], with added disturbance can be obtained as follows:

$$\dot{\boldsymbol{x}}\,(t) = \boldsymbol{A}\,(t)\,x\,(t)) + \boldsymbol{B}(\,t)\,u(t) + \boldsymbol{F}(t)\,d(t)$$

$$\boldsymbol{y}\,(t) = C\,(t)\,x\,(t) \tag{4.19}$$

where

$$\boldsymbol{x}(t) = \begin{bmatrix} \boldsymbol{x}_1(t) \\ \boldsymbol{x}_2(t) \\ \vdots \\ \boldsymbol{x}_N(t) \end{bmatrix},\ u(t) = \begin{bmatrix} \boldsymbol{u}_1(t) \\ \boldsymbol{u}_2(t) \\ \vdots \\ \boldsymbol{u}_N(t) \end{bmatrix},\ \boldsymbol{d}(t) = \begin{bmatrix} d_1(t) \\ d_2(t) \\ \vdots \\ d_N(t) \end{bmatrix}, \boldsymbol{y}(t) = \begin{bmatrix} \boldsymbol{y}_1(t) \\ \boldsymbol{y}_2(t) \\ \vdots \\ \boldsymbol{y}_N(t) \end{bmatrix}. \quad (4.20)$$

Zero-order hold (ZOH) is applied to discretize the continuous-time linear system (CTL) of (4.19) and (4.20) into the distributed discrete-time linear model (state-space) for each control area of the power system and can be expressed as follows [71]:

$$x_i\ (k+1) = \tilde{A}_{ii}\ (k)\ x_i\ (k) + \tilde{B}_{ii}\ (k)\ u_i(k) + \sum_{j\neq i}^{N} (\tilde{A}_{ij}\ (k)\ x_j(k) + \tilde{B}_{ij}\ (k)\ u_j(\mathrm{k}))$$

$$y_i\ (k) = \tilde{C}_{ii}\ x_i\ (k). \quad (4.21)$$

4.2 Algorithm for robust DMPC

In this study, the minimum-maximum problem to be optimized is done locally for every subsystem as in [71], using the distributed discrete-time linear state-space model of (4.21) and represented as shown in (4.22)

$$\min_{u_i(k+\mathrm{p}|k\ l)} \max_{[\tilde{A}_{ii}\ (k+\mathrm{p}\ l)\ \tilde{B}_{ii}\ (k+\mathrm{p}\ l)\cdots\ \tilde{A}_{ij}\ (k+\mathrm{p}\ l)\ \tilde{B}_{ij}\ (k+\mathrm{p}\ l)\cdots],\ l\ \geq 0} J_i(k) \quad (4.22)$$

$$\text{s.t.} \quad |u_i\ (k+\mathrm{p}|k\ l)| \leq u_i^{\max},\ \geq 0$$

Where $J_i\ (k)$ is the objective function for each local subsystem i which guarantees the cooperation of all subsystem controllers and it is defined as [71]

$$J_i(k\ ) = \sum_{l=0}^{\infty} [x_i'(k+p|k\ )\ S_i x_i\ (k+p|k\ ) + u_i'\ (k+p|k\ )\ R_i\ u_i\ (k+|k\ )] + \sum_{j\neq i}^{N} \sum_{l=0}^{\infty} [x_i'\ (k+p|k)\ S_j x_j\ (k+p|k\ ) + u_j'\ (k+p|k\ )\ R_j\ u_j\ (k+p|k\ )] \quad (4.23)$$

where $x_i(k+l\,|\,k)$ is the predicted state, $u_i((k+l\,|\,k)$ is the input variable for the i-th subsystem at time instant $k+l$, $l \geq 0$, based on information at time k. S_i, R_i, S_j, and R_j are the weighting matrices (and they are all positive). The objective function of (4.23) considers the objectives of every controller as depicted by the summation term in the right-hand sum, the superscript "l" previous iteration. The maximization task here is to choose a time-varying model $[\tilde{A}_{ii}\ (k+\mathrm{p}\ )\ \tilde{B}_{ii}\ (k+\mathrm{p}\ )\ \cdots\tilde{A}_{ij}\ (k+\mathrm{p}\ )\ \tilde{B}_{ij}(k+\mathrm{p}\ )\ ...]$ within the uncertainty set Ω to get the worst-case condition of $J_i(k)$, and then the minimization procedure is carried out on this worst-case condition over current and future horizons [71].

To resolve the problem of optimization of (4.22), an upper limit referred to as upper bound of the objective function of (4.23) must be sought for and to achieve it, an assumption is made that there exists a quadratic function as in [61,71]

$$V_i(\bar{x}) = \bar{x}^T P_i \bar{x}, \quad P_i > 0, \tag{4.24}$$

where $\bar{x} = [x_i' x_i' \cdots x_N']'$ is subsystem i vector states having states x_{ii} that can be estimated locally supported with states x_{ij} and those measured and communicated in and among the other subsystem. For all the subsystem i, $V_i(\bar{x})$ should satisfy the following stability constraint similar to [71]:

$$V_i(\bar{x}(k+p+1|k)) - V_i(\bar{x}(k+p|k)) \leq -[x_i'(k+p|k) S_i x_i(k+p|k) + u_i'(k+p|k) R_i u_i(k+p|k)$$

$$+ \sum_{j\neq i}^{N} (x_j'(k+p|k) S_j x_j(k+p|k) + u_j^{l}(k+p|k) R_j u_j(k+p|k))], \; l \geq 0 \tag{4.25}$$

For $l = 0, 1, \ldots, \infty$, the accumulation of (4.25) is

$$V_i(\bar{x}(k|k)) \geq J_i(k) \tag{4.26}$$

Thus, in [1], the upper bound of object function is proven to be

$$\max_{[\tilde{A}_{ii}(k+p)\,\tilde{B}_{ii}(k+p)\cdots\tilde{A}_{ij}(k+p)\,\tilde{B}_{ij}(k+p)\ldots],\, l \geq 0} J_i(k) \leq V_i(x(k|k)) \tag{4.27}$$

A look at the objective function in (4.23) shows that there will be the problem of finding infinite u_i for the infinite time horizon which will result in long computation and impractical polynomial-time solution, hence state-feedback law is sought for and applied to each local and its neighbouring subsystems and u_i is expressed as:

For local subsystem similar to [71]

$$u_i(k+p|k) = f_{ii} x_{ii}(k+p|k) + \sum_{j\neq i}^{N} f_{ij} x_j(k+p|k) = f_i \bar{x}(k+p|k) \tag{4.28}$$

For neighbouring subsystem [61]

$$u_j(k+l|k) = f^*_{jj} x_j(k+l|k) + \sum_{j\neq s}^{N} f^*_{js} x_s(k+l|k) = f^*_j \bar{x}(k+l|k) \tag{4.29}$$

where $f^*_j = [f^*_{j1}\, f^*_{j2} \cdots f^*_{jN}]$.

With the above adjustment, the RDMPC algorithm needs to be re-adjusted based on the state feedback law of (4.28) in [71], the minimization of the upper bound is expressed as.

$$\min_{u_{i(k+l|k)}} V_i(\bar{x}(k|k)) = \min_{f_i} \bar{x}^{l}(k|k)\, P_i \bar{x}(k|k), \qquad P_i > 0. \tag{4.30}$$

Thus, *x* bar expression for the whole power system similar in [61], it becomes

$$\bar{x}\,(k{+}1) = \begin{bmatrix} x_1\,(k+1) \\ x_2\,(k+1) \\ \vdots \\ x_N\,(k+1) \end{bmatrix} = \begin{bmatrix} \tilde{A}_{11}(k) & \tilde{A}_{12}(k) \cdots \tilde{A}_{1N}(k) \\ \tilde{A}_{21}\,(k) & \tilde{A}_{22}\,(k) \cdots \tilde{A}_{2N}\,(k) \\ & \vdots \\ \tilde{A}_{N1}\,(k) & \tilde{A}_{N2}\,(k) \cdots \tilde{A}_{NN}\,(k) \end{bmatrix} \begin{bmatrix} x_1(k) \\ x_1(k) \\ \vdots \\ x_N(k) \end{bmatrix}$$

$$+ \begin{bmatrix} \tilde{B}_{11}(k) \\ \tilde{B}_{21}(k) \\ \vdots \\ \tilde{B}_{N1}(k) \end{bmatrix} u_1(k) + \begin{bmatrix} \tilde{B}_{12}(k) \\ \tilde{B}_{22}(k) \\ \vdots \\ \tilde{B}_{N2}(k) \end{bmatrix} u_2(k) + \ldots + \begin{bmatrix} \tilde{B}_{12}(k) \\ \tilde{B}_{22N}(k) \\ \vdots \\ \tilde{B}_{NN}(k) \end{bmatrix} u_2(k) \qquad (4.31)$$

Define

$$A\,(k) = \begin{bmatrix} \tilde{A}_{11}(k) & \tilde{A}_{12}(k) \cdots \tilde{A}_{1N}(k) \\ \tilde{A}_{21}\,(k) & \tilde{A}_{22}\,(k) \cdots \tilde{A}_{2N}\,(k) \\ & \vdots \\ \tilde{A}_{N1}\,(k) & \tilde{A}_{N2}\,(k) \cdots \tilde{A}_{NN}\,(k) \end{bmatrix} \qquad (4.32)$$

$$B_i(k) = \begin{bmatrix} \tilde{B}_{11}(k) \\ \tilde{B}_{21}(k) \\ \vdots \\ \tilde{B}_{N1}1(k) \end{bmatrix} \qquad (4.33)$$

Substituting, (4.28) and (4.29), the state (4.31) in (4.21), the resulting closed-loop model can be simplified as

$$\bar{x}\,(k{+}1) = [\bar{A}(k) + B_i\,(k)\,f_i]\,\bar{x}\,(k) \qquad (4.34)$$

where

$$\bar{A}\,(k) = A\,(k) + \sum_{j\neq i}^{N} Bj(k) f_j^{*}$$

The robust stability constraint in (4.25) becomes

$$[\bar{A}^{(\ell)}(k{+}p) + Bi^{(\ell)}(k{+}p)\,f_{i]1} \times P_i\,[\bar{A}^{(\ell)}(k{+}p) + Bi^{(\ell)}\,(k{+}p)\,f_i] - P_i$$

$$\leq -\,(\,\bar{S}_i + \sum_{j\neq i}^{N} f_j^{*l} R_j f_j^{*} + f_i' R_i f_i\,) \qquad (4.35)$$

where

$$\bar{S}i = \begin{bmatrix} S_1 & & \\ & S_2 & \\ & & \ddots\ S_N \end{bmatrix}$$

So, a new upper bound can be given as in [61],

$J_i(k) \leq \ V_i\ (\bar{x}\ (\mathrm{k|k})) \leq\ Y_i$

In [71], the optimal problem of (4.9) is equivalent to

$\min_{\gamma_i\,,P_i} \quad \gamma_i$

subject to $\bar{x}'\ (k|k)\ P_i\bar{x}\ (k|k) \leq \gamma_I$ (4.36)

Substituting $P_i = \gamma_i Q_i^{-1}>0,\ Y_i = f_i Q_i,$ and looking at the input constraints of (4.22) coupled with the stability constraint of (4.35) and performing a Schur complement decomposition, minimization problem (4.36) can replace the minimization of $J_i(k)$ as expressed in [61], and linear minimization problem with LMI constraints gives:

$\min_{\gamma_i P_i\, Q_i} \quad \gamma_i$

subject to $\begin{bmatrix} 1 & \bar{x}\ (\mathrm{k|k}) \\ \bar{x}\ (\mathrm{k|k}) & Qi \end{bmatrix} \geq 0,$

$$\begin{bmatrix} Q_i & Q_i\bar{A}_i^{\,i(e)} + Y_i'\ B_i'^{(e)} & Q_i\bar{S}_i^{\,1/2} & Y_iR_i^{1/2} \\ \bar{A}_i^{\,(e)}Q_{i+}\ B_i^{(e)}Y_i & Q_i & 0 & 0 \\ \bar{S}_i^{\,1/2}Q_i & 0 & \gamma_i I & 0 \\ R_i^{1/2}Y_i & 0 & 0 & \gamma_i I \end{bmatrix} \geq 0 \qquad (4.37a)$$

e =1, 2,…L,

$$\begin{bmatrix} (\mathrm{u_i^{max}})^2 I & Y_i \\ Y_i' & Q_i \end{bmatrix} \geq 0. \qquad (4.37b)$$

For the constraints on power system state

$$\begin{matrix} max \\ [\tilde{A}_{ii}\ (k+\mathrm{p})\tilde{B}_{ii}(k+\mathrm{p}) \cdots \tilde{A}_{ij}(k+\mathrm{p})\ \tilde{B}_{ij}(k+\mathrm{p})\ \ldots] \end{matrix} \quad \begin{matrix} \| y_i\ (k+p|k)\ \|_2 \leq y_{i,\max} \\ \in \Omega\ ,\ p\ \geq 0 \end{matrix} \qquad (4.38)$$

Transform it to LMI as

$$\begin{bmatrix} Q_i & \left(\bar{A}_i{}^{(e)} Q_{i+} B_i^{(e)} Y_i\right)' \ \tilde{C}_{ii}' \\ \tilde{C}_{ii}\left(\bar{A}_i{}^{(e)} Q_{i+} B_i^{(e)} Y_i\right) & Y_i^2, max^I \end{bmatrix} \geq 0 \qquad (4.39)$$

$$e = 1, 2, \ldots, L,$$

The steps for implementing the procedure for the LMI optimization are;

Step 1**:** This is the initialization phase where control interval $k=0$ or $t = 0$ and set $F_i=0$. Also enter the weight matrix for *A, B, C, D, S, Q* and other given or known parameters.

Step 2: This is the updating phase at the start when iteration is set at $t=0$ and $F_i = F_i^{(0)}$ for all subsystem controllers upon which they all exchange their local state data and initial estimates.

Step 3: This step is to carry out LMI iterations for $t \leq T_{max}$ and solve LMI problems (4.39) in parallel to get the minimizers values for $Y_i^{(t)}$, $Q_i^{(t)}$ to aid in estimating the feedback solutions $F_i^{(t)} = Y'^{(t)} Q_i^{-1(t)}$ a check is done for feasibility, if infeasible set $F_i^{(t)} = F_i^{(t-1)}$

Check the invariant ellipsoid and Lyapunov matrix using matrix $\begin{bmatrix} 1 & \bar{x}\ (\mathrm{k|k}) \\ \bar{x}\ (\mathrm{k|k}) & Qi \end{bmatrix} \geq 0$

Enter input and output constraints using the matrix equation (4.37a)

Apply the feedback control law, optimize by adding the step results above and run robustness using $F = YQ^{-1}$.

Finally, run the closed-loop performance by substituting into the discrete state-space equation of (4.37b) to get output y_i value.

If $|| F_i^{(t)} - F_i^{(t-1)} || \leq \varepsilon_i$, for all I = 1…N

Break

end if

Exchange the solutions *Fi's* and set $t = t + 1$

end while

Step 4: Apply $u_i = F_i x_i$ to the subsystems, the control interval $k = k + 1$ is then increased, repeat the procedures from step 1.

4.3 Simulationand test results

In this section, two-area hydro-thermal power system, where CA 1 is the thermal power plant, CA 2 is the hydropower plant, likewise the three areas hydro-thermal power system, where CA 1

and CA 2 are thermal power plant and CA 3 is hydropower plant as shown in Figure 4-1 and 4-2. Simulations are done for LFC with RDMPC algorithm and conventional PID controller, stability and the robustness performance for the proposed RDMP are analysed using MATLAB toolbox and MATLAB LMI Solver. A load change was introduced at t = 0.2 s and span to 2 s with ΔP_{L1} set at 0. 01p.u MW and a sampling time T_s of 0.1 s. The parameters used for proportional gain is 0.8, integral gain is 5 and 0.2 for derivative, for LMI algorithm Q=1, R=0.01 and γ = 1. The parameter variable used is given in Table A-2(Appendix A).

4.3.1 Case 1; Load disturbance for two-area hydro-thermal power system

The MATLAB/Simulink model of the two-area hydro-thermal system is shown in Figures 4-3 and 4-4. The effectiveness of the controllers is checked using the proposed RDMPC and compared with PID controllers for frequency deviation Δf_1, Δf_2, area control error ACE_1 and ACE_2, load disturbance was initiated, the tie-line point was set at 100% participation from the neighbouring power plant. Figures 4-5 and 4-6, show the corresponding dynamic response result as PID (red line) while RDMP as (blue line). RDMPC controllers show good dynamic response compare to PID when compare since it MPCs controllers interact with each other to achieve an optimal result.

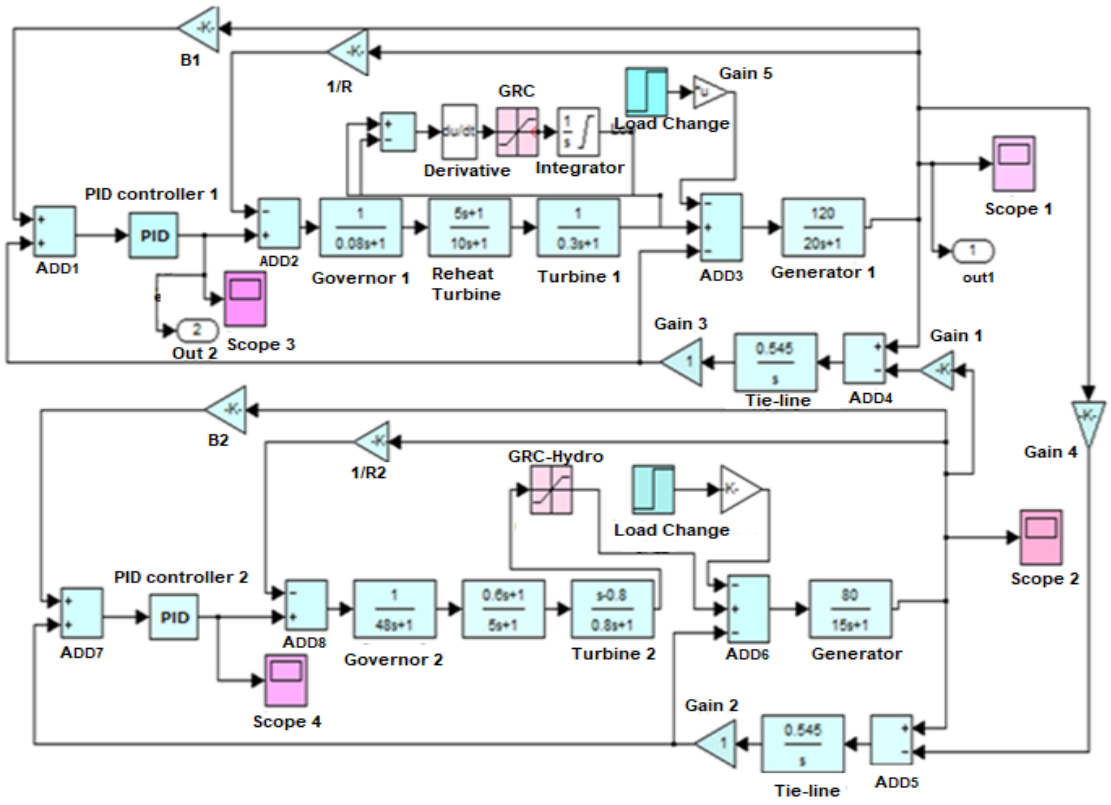

Figure 4-3 Simulink model of a two-area hydro-thermal power system with GRC and PID

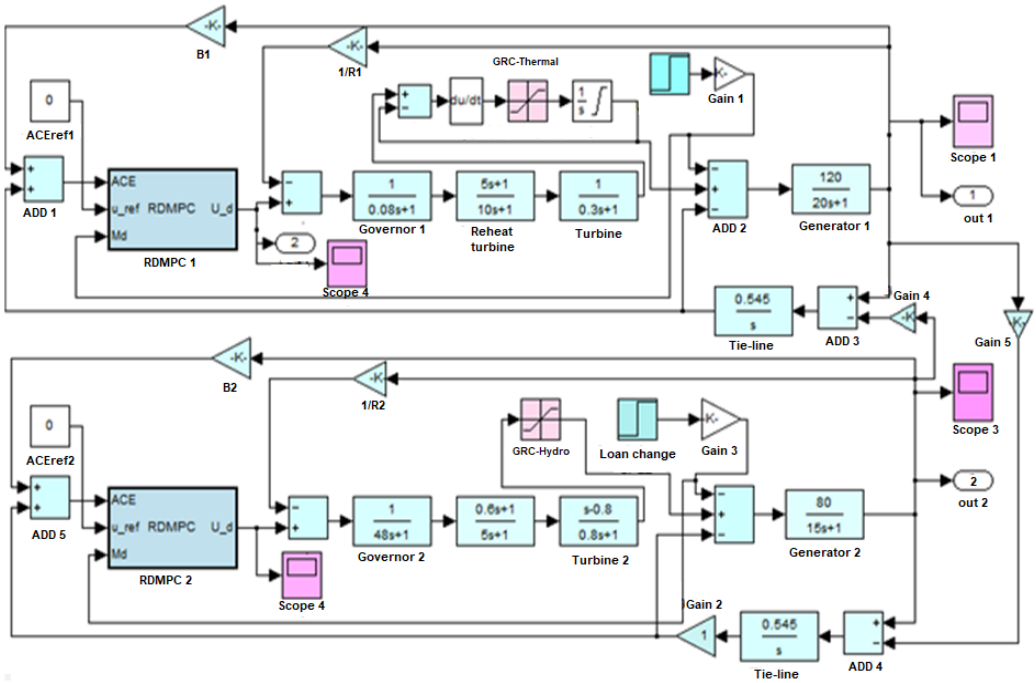

Figure 4-4 Simulink model of a two-area hydro-thermal power system with RDMPC

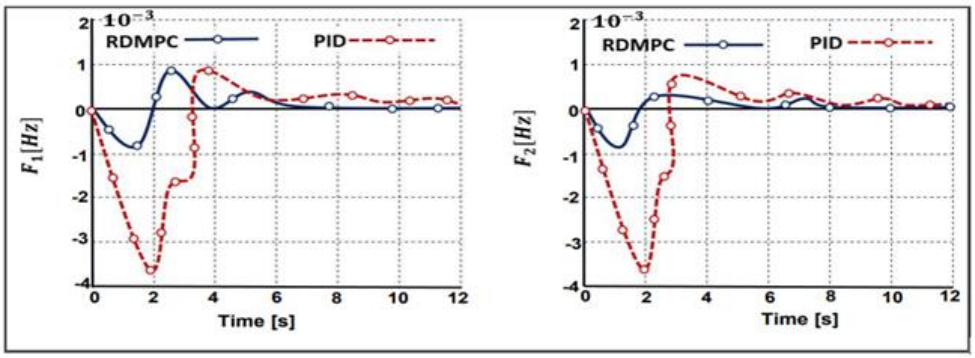

Figure 4-5 Frequency deviation in two area power system

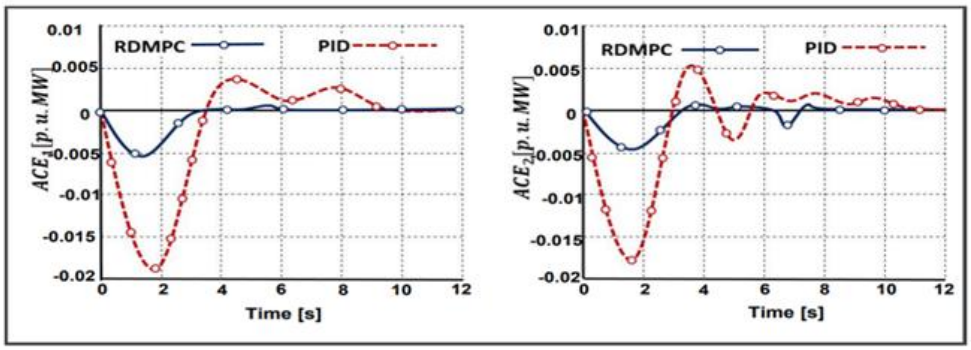

Figure 4-6 ACE signal in two area power system

4.3.2 Case 2; Load disturbance in three-area hydro-thermal power system

The MATLAB/Simulink model of the three-area hydro-thermal power system in a subsystem form is shown in Figure 4-7. Power contributions from the tie-line point were set at 50% participation from the neighbouring power plant, a load change was introduced, the dynamic response of frequency deviation $\Delta f_1, \Delta f_2, \Delta f_3$, area control error ACE_1 and ACE_2, ACE_3. The signal are clearly demonstrated by Figures 4-8 and 4-9. The dynamic response graph of the power system clearly shows that RDMPC is more robust when compared with conventional PID controller, as it tracks the load disturbance change as shown by the amplitude. The response shows the advantages of the RDMPC when tuned for hard constraint levels in a complex power system over the conventional PID.

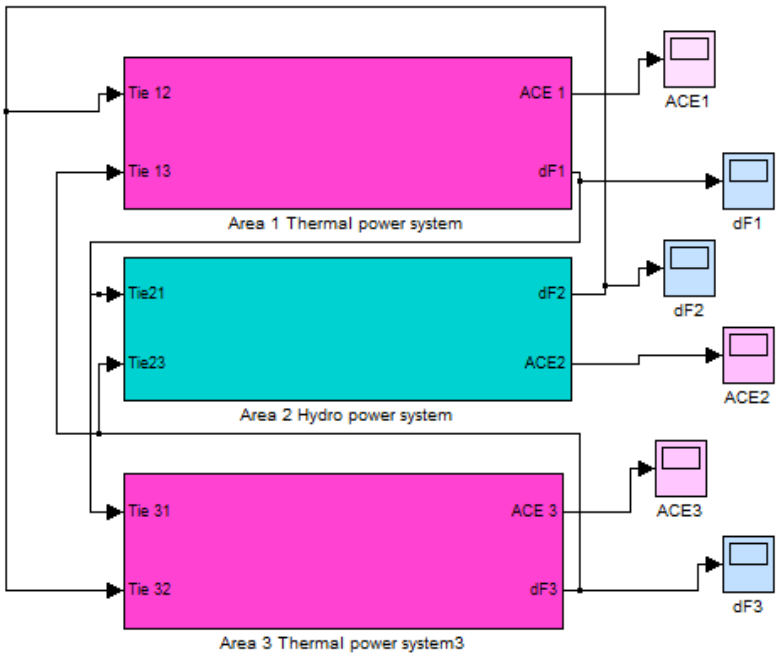

Figure 4-7 Simulink model of the three-area power system in subsystem form

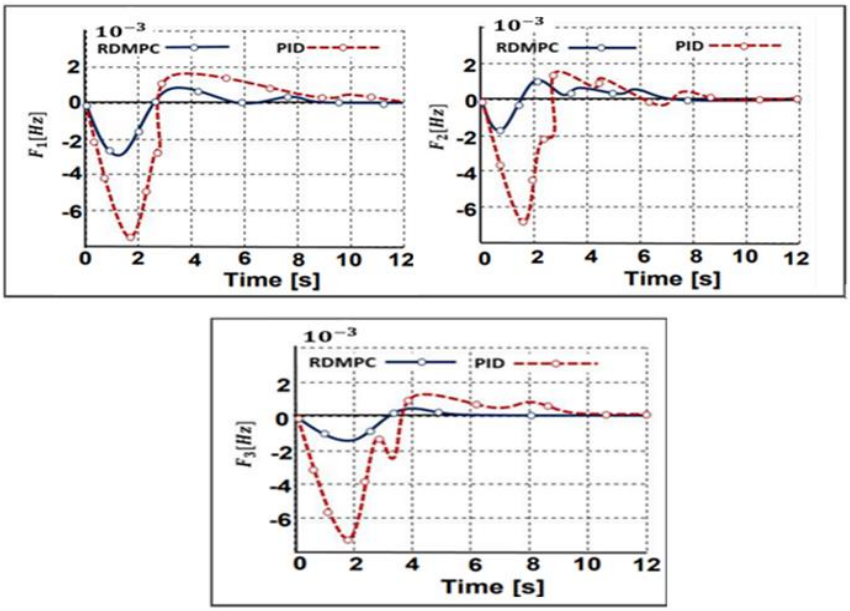

Figure 4-8 Frequency deviation in the three-area power system

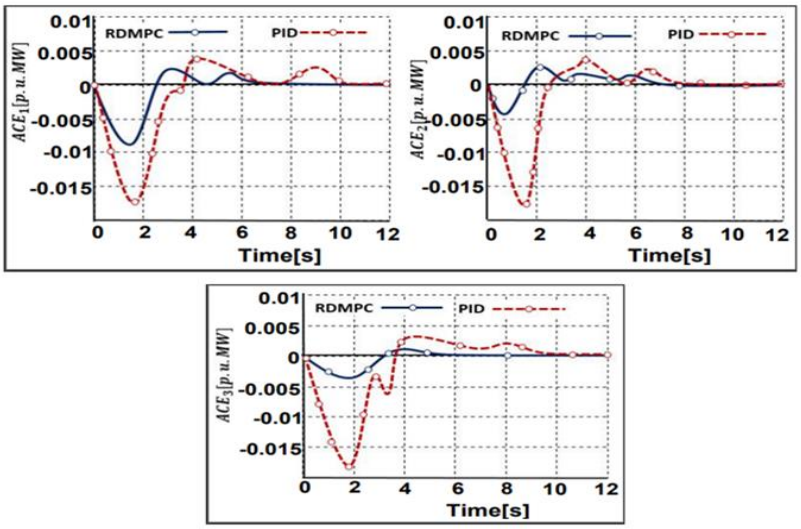

Figure 4-9 ACE signal in the three-area power system

4.4 Chapter conclusion

In this chapter, the RDMPC algorithm for LFC control for a two-area and three-area hydro-thermal IPS were presented. The formulation of RDMPC algorithm and mathematical expressions were presented and how the upper bound was derived and a feedback control law applied to force the input variable and state parameters from getting to the upper bound levels, the resulting LMI equations were presented for optimization of system parameters for better tracking and convergence feasibility. The algorithm was tested with two- area and three-area hydro-thermal

plants respectively. The simulation results prove that RDMPC is more robust and has a better dynamic response when compared to PID.

Although RDMPC successfully take care of system by bringing the frequency and ACE to optimal, which is an effective way of controlling frequency deviation for a robust interconnected power system, it is observed that the response still lags, from the amplitude obtained from in the signals of RDMPC, hence this can be improved upon by developing an adaptive MPC, using AMPC to check the system error and help in faster response in the power system network. In chapter five, an adaptive MPC is presented as an improvement to help in the effective tracking, faster dynamic response and better steady-state equilibrium of uncertainties in parameters and load change by being able to adapt its objective function to suit expected response. Finally, the robustness of the AMPC is analysed in the presence of multiple load disturbances, non-linearity constrains and robustness tests for parameter change from the neighbouring subsystem after readjustment of the adaptive MPC system. Comparative performance between AMPC, RDMPC and conventional PID are analysed.

CHAPTER 5

DEVELOPMENT OF AN ADAPTIVE MPC

5.0 Adaptive robust predictive control

In chapter four, the advantages of using the robust distributed model predictive control algorithm over conventional PID controllers are established. Despite the obvious advantages, the RDMPC algorithm presented in chapter four still has some limitations from the system varying dynamics and uncertainties. This is because in the development and analysis of RDMPC it was assumed that the internal plant state matrices were constant (i.e. matrices *A, B,* and *C*) just like the traditional MPC despite its robustness. This constant state model assumption makes it poor in handling plant varying dynamics which constantly changes operating conditions for every time step.

The solution to this inadequacy is the introduction of AMPC controller that has dynamic characteristics that change with the system plant changing dynamics and uncertainties that effectively track the changing operating points. An adaptive MPC is proposed in this chapter, that provides a new linear plant model for each time step as operating conditions changes during the prediction horizon duration, therefore presenting more accurate predictions for the new and emerging operating conditions.

The design of adaptive nonlinear MPC schemes is changeling for IPS as a result of the separation principle assumption widely utilized in linear control systems is not applicable to a general category of nonlinear systems, within the presence of constraints [98]. There are only few results on adaptive MPC for LFC control literature in the last decade [92]. Real adaptive nonlinear MPC algorithm of power system addresses the difficulty of robustness to model uncertainty while the estimator is evolving [98]. Unfortunately, this may not be achieved without introducing expanded state vector, and optimization of control signal vector in the controller [92,93].

5.1 Dynamic model of interconnected power plant

In chapter four, the general CTL system with added disturbance for the whole power system state-space equation was given as follows according to [71]:

$$\dot{\boldsymbol{x}}(t) = \boldsymbol{A}(t)\,\boldsymbol{x}(t)) + \boldsymbol{B}(t)\,\boldsymbol{u}(t) + \boldsymbol{F}(t)\,\boldsymbol{d}(t)$$

$$\boldsymbol{y}(t) = \boldsymbol{C}(t)\,\boldsymbol{x}(t) \qquad (5.1)$$

The state vector $\boldsymbol{x}(t)$, the control vector $\boldsymbol{u}(t)$, the disturbance vector $\boldsymbol{F}(t)$ and system output vector $\boldsymbol{y}(t)$ for the power plants were presented in chapter four with the state parameter matrices. For adaptive MPC application the CTL is discretized by applying zero-order hold (ZOH) discretization and this result in the following distributed discrete-time linear model (state-space) which applies to two and three area power system based on the work of [61, 71]:

$$\boldsymbol{x_i}(k+1) = \tilde{\boldsymbol{A}}_{ii}(k)\,\boldsymbol{x}_i(k) + \tilde{\boldsymbol{B}}_{ii}(k)\,\boldsymbol{u}_i(k) + \boldsymbol{F}_i d(k) + \sum_{j\neq i}^{N}(\tilde{\boldsymbol{A}}ij(k)\,\boldsymbol{x}_j(k) + \boldsymbol{B}_{ij}(k)\,\boldsymbol{u}_j(k))$$

$$\boldsymbol{y}_i(k) = \tilde{\boldsymbol{C}}_{ii}\,\boldsymbol{x}_i(k). \qquad (5.2)$$

In [92], where $\boldsymbol{A_f} = e^{AT_s}, \boldsymbol{B_f} = \int_0^{T_s} e^{At}\,\boldsymbol{B}dt, \boldsymbol{B_{If}} = \int_0^{T_s} e^{At}\,\boldsymbol{B_I}dt$. This discrete model is then used in the following controller design in the MPC framework. The incremental form of (5.2) according to [92] is defined as follows:

$$\Delta\boldsymbol{x}(k+1) = \mathbf{A}_{\boldsymbol{f}}\Delta\boldsymbol{x}(k) + \mathbf{B}_{\boldsymbol{f}}\Delta\boldsymbol{u}(k) + \mathbf{B}_{\boldsymbol{I}}\Delta\boldsymbol{u_I}(k)$$

$$\Delta\boldsymbol{y}(k) = \boldsymbol{C}\Delta\boldsymbol{x}(k) \qquad (5.3)$$

where $\Delta\boldsymbol{x}(k+1)$, $\Delta\boldsymbol{x}(k)$, $\Delta\boldsymbol{u}(k)$, $\Delta\boldsymbol{u_I}(k)$, and $\Delta\boldsymbol{y}(k)$ are the incremental forms of $\boldsymbol{x}(k+1)$, $\boldsymbol{x}(k)$, $\boldsymbol{u}(k)$, $\boldsymbol{u_I}(k)$, and $y(k)$, respectively and follows for the neighbour subsystem contribution is denoted as ij. Using the two-area hydro-thermal power system as a reference model for the optimization of the control signal vectors, by minimizing the weighted sum of square predicted errors and square future control values [92]. Figure 5-1 shows the block diagram of two areas hydro-thermal power system with AMPC controller.

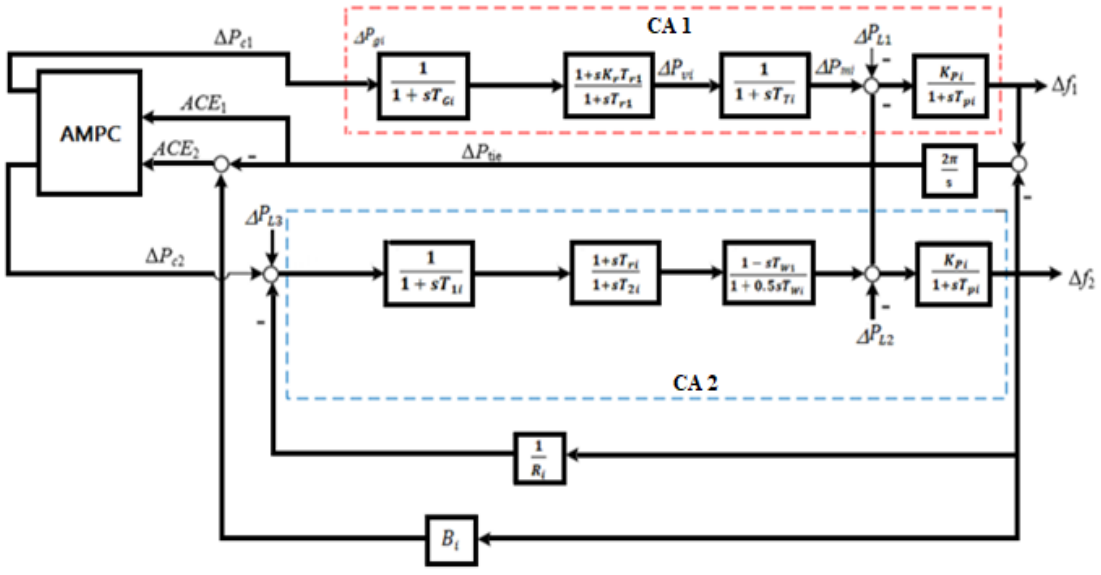

Figure 5-1 Two-area hydro-thermal power system with AMPC controller [62]

5.2 Proposed AMPC controller design

An adaptive MPC controller is proposed to achieve the closed-loop stability and fast-tracking of two-area and three-area hydro-thermal power system constrain. The main ideal of the AMPC control for constrained systems is mainly focused on improving the performance of RDMPC as showed in chapter 4, by eliminating dynamics and uncertainties with the adapted models, while constraints are satisfied robustly [94]. In AMPC the dynamic predictive model is established by introducing an expanded state vector and optimization of control signal vector base on the cost function, by minimizing the weighted sum of the square predicted error and square feature control values [92]. Figure 5-2 shows the block diagram of the proposed adaptive MPC for an interconnected power system.

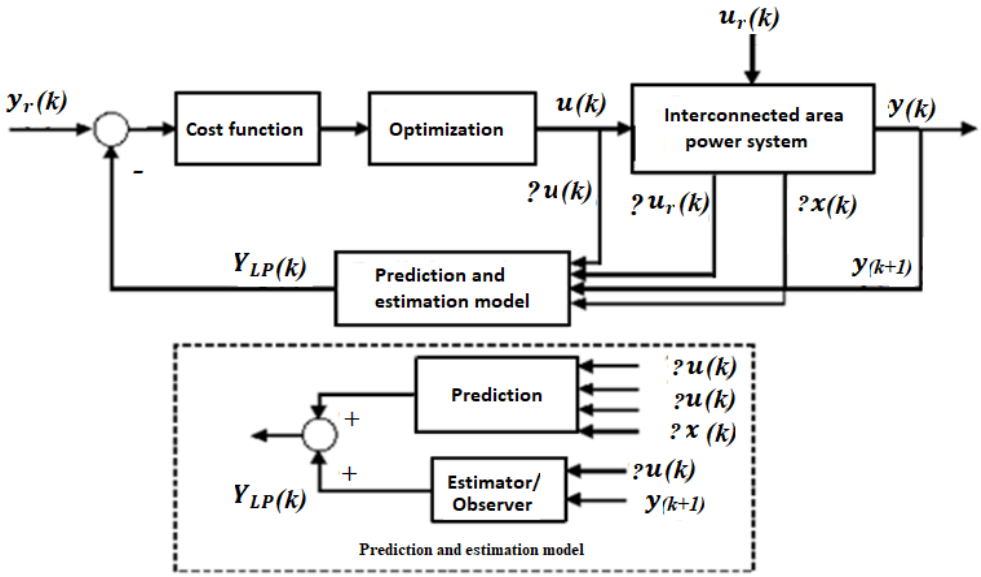

Figure 5-2 Block diagram of the proposed adaptive MPC method for LFC [62].

5.2.1 Formulation of the prediction problem

The major objective of the power plant LFC system to restore frequency deviations, ACE, and tie-line active power deviation to back the desired level quickly to prevent system failure due to oscillations [95]. The concept of the proposed method is obtained by predicting how the future states will be for Y, $\Delta \boldsymbol{x}$, and $\Delta \boldsymbol{U}$. According to (5.3), in [92], the state variable discrepancy is given as

$$\Delta \boldsymbol{x}(k+1) = \boldsymbol{x}(k+1) - \boldsymbol{x}(k);$$

$$\Delta \boldsymbol{x}(k) = \boldsymbol{x}(k) - \boldsymbol{x}(k-1),$$

The control variable discrepancy by $\Delta \boldsymbol{u}(k) = \boldsymbol{u}(k) - \boldsymbol{u}(k-1)$. These are the increase in the variables **x**(k) and $\boldsymbol{u}(k)$. Connect input $\Delta \boldsymbol{x}(k)$ to the output $y(k)$. Then a new state variable vector is established an extended state vector similar to [92], expressed as;

$$\boldsymbol{W}(k) = [\Delta \boldsymbol{x}(k) \text{ y } (k+1)]^T,$$

Then in (5.2) and (5.3) used to reformulate the expanded discrete-time state-space model similar in [92], is given as:

$$\boldsymbol{W}(k+1) = \boldsymbol{L}\boldsymbol{W}(k) + \boldsymbol{M}\Delta \boldsymbol{u}(k) + \boldsymbol{M_I}\Delta \boldsymbol{u_I}(k)$$

$$\boldsymbol{y}(k) = \boldsymbol{B_z}\boldsymbol{Z}(k) \tag{5.4}$$

Where $\boldsymbol{L} = \begin{bmatrix} \boldsymbol{A_f} & \boldsymbol{0}_{H_{x*}H_y} \\ \boldsymbol{C} & \boldsymbol{E}_{H_y} \end{bmatrix}_{(x+Ny)(Nx+Ny)}$,

$$\boldsymbol{M} = \begin{bmatrix} \boldsymbol{B_f} \\ \boldsymbol{0}_{H_{y*}H_u} \end{bmatrix}_{(H_x+Hy)H_u},$$

$$\boldsymbol{M_I} = \begin{bmatrix} \boldsymbol{B_{If}} \\ \boldsymbol{0}_{H_{y*}H_{uI}} \end{bmatrix}_{(H_x+H_y)N_{uI}},$$

$$\mathbf{B_Z} = \begin{bmatrix} \mathbf{C} & \mathbf{E}_{\mathrm{H_y}} \end{bmatrix}_{\mathrm{H_y(H_x+Hy)}} . \tag{5.5}$$

An identity matrix is given as E_{H_y} with H_y denote as column and row matric, then $\boldsymbol{0}_{H_{x*}H_y}$ is zero matrics with H_y column, H_x rows, H_y, H_{uI}, H_x and H_u are the states number of $\boldsymbol{y}(t)$, $\boldsymbol{u_I}(t)$, $\boldsymbol{u}(t)$ and $\boldsymbol{u}(t)$, accordingly. The predictive output value $\boldsymbol{y}(k+p|k)$ at k-th sample time is formulated as [92]:

$$\boldsymbol{y}(k+p|k) = \boldsymbol{B_z}\boldsymbol{L^p}\boldsymbol{Z}(k) + \sum_{j=1}^{p} \boldsymbol{B_z}\boldsymbol{L}^{p-j}\boldsymbol{M}\Delta \boldsymbol{u}(k+j-1) + \sum_{j=1}^{p} \boldsymbol{B_z}\boldsymbol{L}^{p-j}\boldsymbol{M_I}\Delta \boldsymbol{u_I}(k+j-1),$$

$$p = 1, 2, \ldots, p, \tag{5.6}$$

where p is prediction horizon, and N is the control horizon. The predictive output vector $\boldsymbol{Y_{LP}}(k)$ similar to [92], is given as follows:

$$\boldsymbol{Y_{LP}}(k) = \Phi \boldsymbol{W}(k) + \psi \Delta \boldsymbol{U}(k) + \psi_I \Delta \boldsymbol{U_I}(k) \tag{5.7}$$

where each vector is defined as follows:

$$\boldsymbol{Y_{LP}}\ (k\ )=\begin{bmatrix} \mathbf{y}(k\ +1(k+1|k\ ) \\ \cdots \\ \mathbf{y}(k\ +1(k+1|\mathrm{k}\ ) \end{bmatrix}_{(PHy)1},$$

$$\Delta\boldsymbol{U}(k)=\begin{bmatrix} \Delta\boldsymbol{u}(k\ ) \\ \cdots \\ \Delta\boldsymbol{u}(k\ +p-1) \end{bmatrix}_{((P\ -H_u)1},$$

$$\Delta\boldsymbol{U_I}(k)=\begin{bmatrix} \Delta\boldsymbol{u_I}(k) \\ \cdots \\ \Delta\boldsymbol{u_I}(k+p-1) \end{bmatrix}_{((\mathrm{P}-\mathrm{H_u})*\mathrm{u_I})1}, \emptyset=\begin{bmatrix} \boldsymbol{B_zL} \\ \boldsymbol{B_zL^2} \\ \vdots \\ \boldsymbol{B_zL^2} \end{bmatrix}_{((PH_y)(u_x+H_y)},$$

$$\Psi=\begin{bmatrix} \boldsymbol{B_zM} & 0_{H_u} & \cdots & \mathbf{0}_{H_u} \\ \boldsymbol{B_zLM} & B_zM & \cdots & \mathbf{0}_{H_u} \\ \vdots & \vdots & \vdots & \vdots \\ \boldsymbol{B_zL^{P-1}M} & \boldsymbol{CB_zL^{P-2}M} & \cdots & \boldsymbol{B_zM} \end{bmatrix}_{((PH_y)((p-1)H_u},$$

$$\psi_I=\begin{bmatrix} \boldsymbol{B_zM_I} & \mathbf{0}_{H_{uI}} & \cdots & 0_{H_{uI}} \\ \boldsymbol{B_zLM_I} & \boldsymbol{BzM_I} & \cdots & 0_{H_{uI}} \\ \vdots & \vdots & \vdots & \vdots \\ \boldsymbol{B_zL^{p-1}M_I} & \boldsymbol{B_zL^{p-2}M_I} & \cdots & \boldsymbol{B_zM_I} \end{bmatrix}_{((P*H_y)((p-1)H_{uI}}.$$

5.2.2 Optimization problem formulation

In the optimization step, the idea is to optimize the control variable change $\Delta\boldsymbol{U}$ and $\boldsymbol{Y_{LP}}(k)$ to be as close to the reference trajectory. In [92], the reference trajectory $\boldsymbol{y_r}(k+p|k)$ is given as follows:

$$\boldsymbol{y_r}\ (k+p|k\ ) = \lambda^p\boldsymbol{y}(k\ ) + (1 - \lambda^p)\ \boldsymbol{c}(k),\ p = 1, \ldots P, \tag{5.8}$$

where λ is a softening factor, and $c(k)$ is the set value of system output. If the data vector that contains the set-point measurement is 1

$\boldsymbol{Y_r}(k)$ = ones [*1 1 1 1*] $y_r(k)$

$$\boldsymbol{Y_r}\ (k\ )=\begin{bmatrix} \boldsymbol{y_r}(k+1|k\ ) \\ \cdots \\ \boldsymbol{y_r}(k+P|k\ ) \end{bmatrix}_{(P*Ny)1} \tag{5.9}$$

The optimal LFC objective of IPS is given as a typical MPC constraint [92]:

$$\min J(k) = \min\{(\boldsymbol{Y_{LP}}(k) - \boldsymbol{Y_r}(k))^T \boldsymbol{S}(\boldsymbol{Y_P}(k) - \boldsymbol{Y_r}(k)) + (\Delta \boldsymbol{U}(k))^T \boldsymbol{R}(\Delta \boldsymbol{U}(k))\}, \quad (5.10)$$

s.t. (5.7)– (5.9)

$$\boldsymbol{u}_{min} \leq \mathbf{u}(\mathrm{k}) \leq \boldsymbol{u}_{max}$$

$$\Delta \boldsymbol{u}_{min} \leq \Delta \mathbf{u}(\mathrm{k}) \leq \Delta \boldsymbol{u}_{max}$$

$$\boldsymbol{y}_{min} \leq \mathbf{y}(\mathrm{k}) \leq \boldsymbol{y}_{max}, \quad (5.11)$$

In general, *S* and *R* weighting vectors can be determined by some empirical rules, and trial and error [92,96].

This shows that the optimal solution of the control signal is linked to the set-point signal $Y_r(k)$ and the state variable $\boldsymbol{W}(k)$ according to the gradient descent method, i.e., $\frac{\partial J(k)}{\Delta U(k)} = 0$, from [92] and [97], the control law $\boldsymbol{u}(k)$ is given as in [92]:

$$\Delta \boldsymbol{U}(k) = (\psi^T \boldsymbol{S} \psi + R)^{-1} \psi^T \boldsymbol{S}(\boldsymbol{Y_r}(k) - \Phi \boldsymbol{W}(k) - \psi_I \Delta \boldsymbol{U_I}(k)), \quad (5.12)$$

$$\Delta \boldsymbol{u}(k) = (E_{H_u} \mathbf{0}_{H_u} (p\text{-}1)) \Delta U(k), \quad (5.13)$$

$$\boldsymbol{u}(k) = \Delta \boldsymbol{u}(k) + \boldsymbol{u}(k - 1). \quad (5.14)$$

AMPC algorithm.

Step 1: Import the discrete-time state-space model described in (5.3) and (5.4), introduce expanded state vector and obtain expanded state-space model described in (5.5).

Step 2: Initialize T_{max} , *p*, *N*, ***S,*** and ***R***, set $k = 1$;

Step 3: For every single time *k*, use the past output vector $y(k\text{-}1) = [ACE_i(k-1)]^{\mathrm{T}}$, control vector $\boldsymbol{u}(k-1) = [\Delta P_{ci}(k-1)]^{\mathrm{T}}$, state vector $\boldsymbol{x}(k-1) = [\Delta f_i(k-1), \Delta P_{tie,i}(k-1)\ \Delta X_{gi}(k-1)$, $\Delta P_{gi}(k-1)]^{\mathrm{T}}$, and disturbance vector $\boldsymbol{u_I}(k - 1) = [\Delta P_{Li}(\mathrm{k}-1)]^{\mathrm{T}}$ depending on the number of interconnected areas.

Step 4: Obtain the predictive vector $\boldsymbol{Y_P}(k)$ by (5.7), control vector $\boldsymbol{u}(k)$ according to (5.12)– (5.14) and the rolling optimization model consisting of the cost function (5.10) and constraints (5.11).

Step 5: Compute the optimal system output $\boldsymbol{y}(k)$ and state vector $\boldsymbol{x}(k)$ under $\boldsymbol{u}(k)$ and set $k = k + 1$ and return step 4 until $k = T_{max}$.

Step 6: Obtain the system output $\{y(k), k = 1, 2, \ldots, T_{max}\}$, frequency deviation $\{[\Delta f_i(k), = 1, 2, \ldots, T_{max}\}$, and tie line power$\{\Delta P_{tie,i}(k), k = 1, 2, \ldots, T_{max}\}$ for IPS.

Remark 1: During the implementation of this control scheme it is important that the neighbouring controllers in each subsystem communicate, share and update information with each other continuously, to archive closed-loop system stability in the AMPC algorithm.

5.3 Simulation and discussion

A simulation study is presented on the two-area and three-area hydro-thermal power system using the same parameters value in chapter 4 as shown in Table A-1(Appendix A), to demonstrate the robustness of the proposed AMPC algorithm and compare with PID which generates the output signal for a correction of proportional and integral error and RDMPC which solve optimization problem using a min-max cost function with LMI methodology in polynomial time. Case studies are presented for two-area and three-area IPS. The simulation for PID, RDMPC, and AMPC are perfumed when a load disturbance of ΔP_L = 0.1 p.u MW at time = 2 s, that span till 4 s and a sampling time of 0.1 s. The parameters used in the PID are proportional gain = 0.8, integral gain = 5 and 0.2 for derivative. The test cases used for the IPS include the following;

1. Multiple load disturbance (two-area hydro-thermal system)
2. Robustness test on parameter change T_T (two-area hydro-thermal power system)
3. Multiple load disturbance (three-area hydro-thermal power system)
4. Robustness test on parameter change T_g (three-area hydro-thermal power system)
5. Downtime uncertainty (three-area hydro-thermal power system)
6. Non-linearity constraint (two-area hydro-thermal system)

5.3.1 Case 1; Multiple load disturbance (two-area hydro-thermal system)

In this section, simulation is used to investigate the proposed AMPC as a result of a multiple load disturbance in the two-area hydro-thermal power system, the control schemes PID, RDMPC, and AMPC are simulated for frequency deviation Δf_1, Δf_2 , area control error ACE_1, ACE_2 and tie-line active power Δp_{tie}. Figure 5-3 to 5-5 shows the response graph as PID (red line), RDMP (blue line) and AMPC (purple line). AMPC has a better and faster dynamic response than the others closely followed by RDMPC. However, all the load reference set point approached zero at steady state.

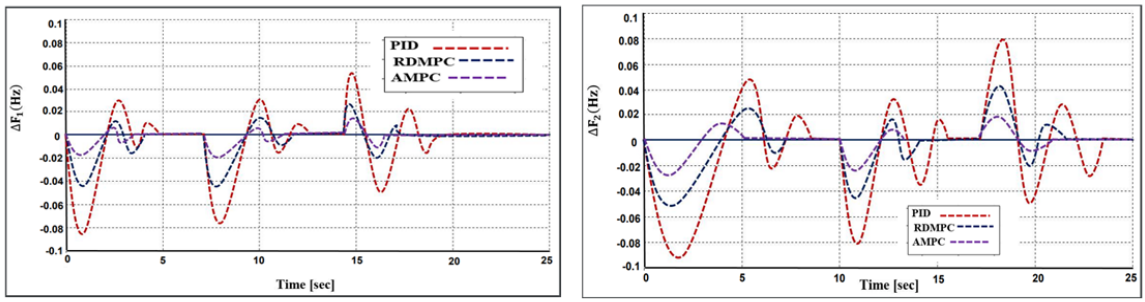

Figure 5-3 Frequency response for area 1 and 2.

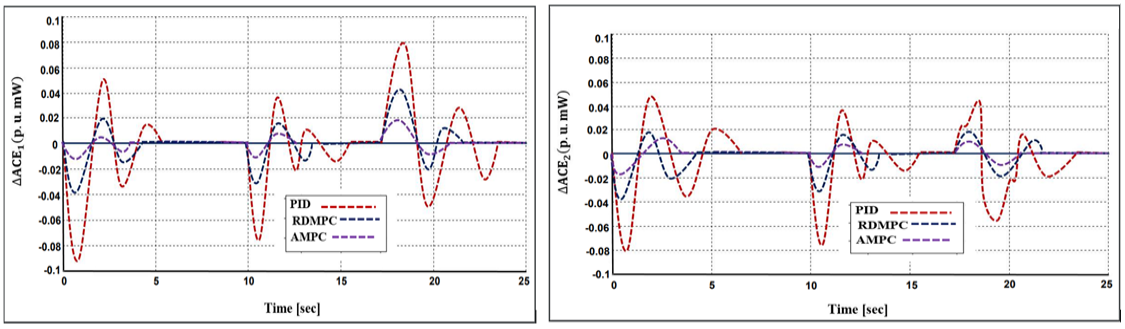

Figure 5-4 Area control error for area 1 and 2.

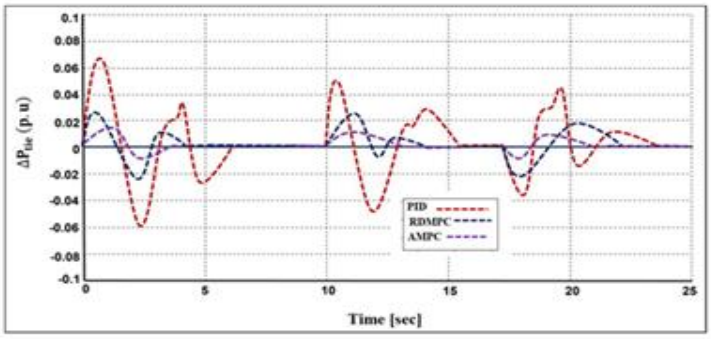

Figure 5-5 Tie-line active power deviations between control area 1 and control area 2

5.3.2 Case 2; Robustness test on parameter change T_T (two-area hydro-thermal power system)

The performance of the controller schemes under two conditions of changing the turbine time constant (T_T) for a 40% increase and a 40% decrease was investigated. The controller schemes PID, RDMPC and AMPC are simulated for frequency deviation Δf_1, Δf_2. Figure 5-6 and 5-7 show dynamic frequency response for a 40% increase and a 40% decrease in T_T parameter

variation respectively. Tables 5-1 and 5-2 show performance indices and percentages improvement. From the comparative analysis, there is a 16.00%, 20.00% and 62.50% improvement on RDMPC in settling time, undershoot and peak overshoot respectively with a 40% increase T_T in CA 1, similarly, there is 26.72%, 48.57% and 50.00% improvement on RDMPC in settling time, undershoot and peak overshoot with 40% decrease T_T in CA 2. This shows the effectiveness of AMPC, with a significant improvement over RDMPC and PID.

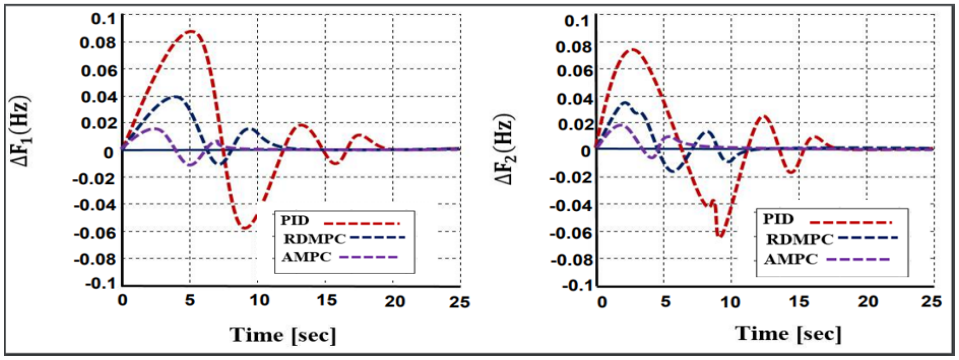

Figure 5-6 Frequency response for a 40% increase in TT parameter variation

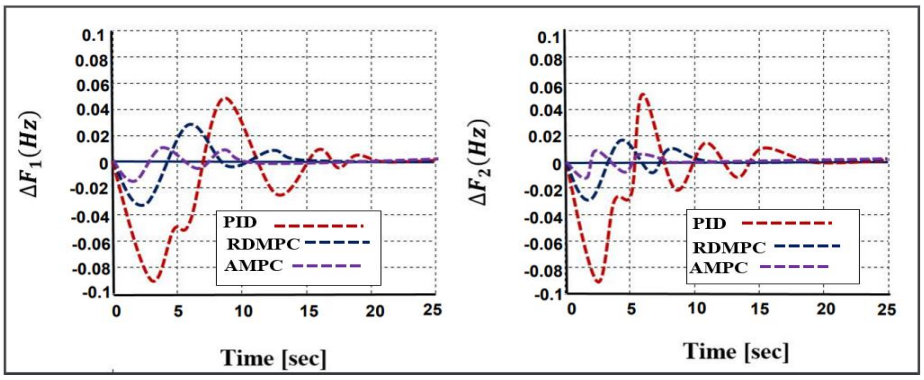

Figure 5-7 Frequency response for 40% decrease in *TT* parameter variation

Table 5-1 Performance comparison for 40% Increase TT parameter variation

System parameters	CA	40% Increase in T_T parameter variation			40% Decrease in T_T parameter variation		
		PID	RDMPC	AMPC	PID	RDMPC	AMPC
Setting time (s)	Δf_1	18.7	12.5	10.5	19.01	15.01	11.00
Undershoot (Pa.MW)	Δf_1	-0.06	-0.012	-0.09	-0.09	-0.035	-0.018
Peak overshoot (p.a MW)	Δf_1	0.088	0.04	0.015	0.053	0.03	0.015
Setting time (s)	Δf_2	18.3	12.4	11.01	18.00	12.01	8.01
Undershoot (Pa.MW)	Δf_2	-0.061	-0.018	-0.011	-0.086	-0.021	-0.01
Peak overshoot (p.a MW)	Δf_2	0.075	0.038	0.02	0.052	0.019	0.01

Table 5-2 Improvement percentage of TT parameter variation

System parameters	CA	% Improvement of AMPC w.r.t PID & RDMPC			
		40% $>$ T_T w.r.t PID	40% $>$ T_T w.r.t RDMPC	40% $<$ T_T w.r.t PID	40% $<$ T_T w.r.t RDMPC
Setting time (s)	Δf_1	43.85	16.00	62.08	26.72
Undershoot (Pa.MW)	Δf_1	80.00	20.00	80.00	48.57
Peak overshoot (p.a MW)	Δf_1	82.95	62.50	71.70	50.00
Setting time (s)	Δf_2	39.84	11.21	55.50	33.31
Undershoot (Pa.MW)	Δf_2	81.97	38.00	88.37	52.38
Peak overshoot (p.a MW)	Δf_2	73.00	47.37	80.77	47.37

5.3.3 Case 3; Multiple load disturbance (three-area hydro-thermal power system)

In this simulation, the same test carried out on the two-area system was done for the three-area power system as a result of a multiple load deviation on the power system. The control schemes AMPC, RDMPC and PID were also considered in the simulated, Figure 5-8 to 5-10 shows the dynamic response graph of the frequency deviation. The closed-loop trajectory of AMPC is distinguishable from the close loop obtain from PID and RDMPC. This satisfies the advantage of proposed AMPC.

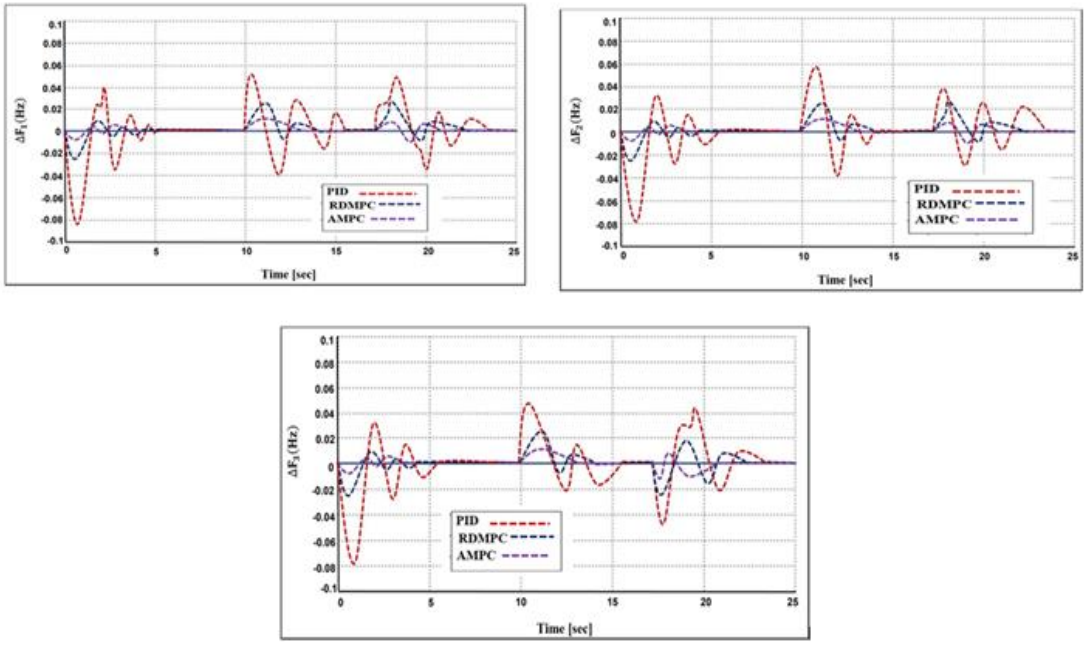

Figure 5-8 Frequency deviations for control area 1, 2 and 3

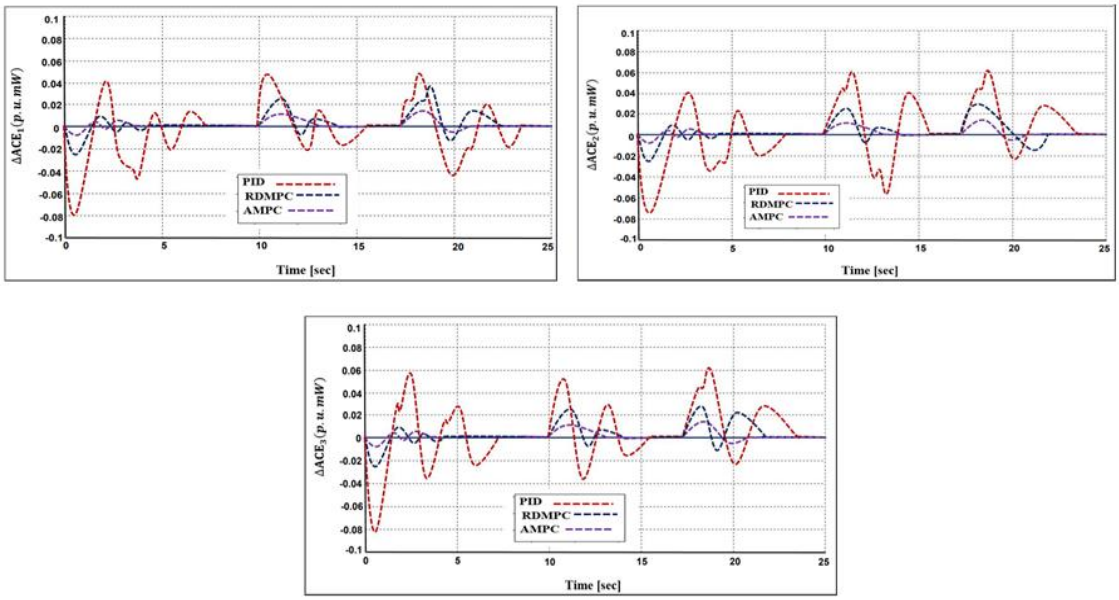

Figure 5-9 Area control error for area 1, 2 and 3

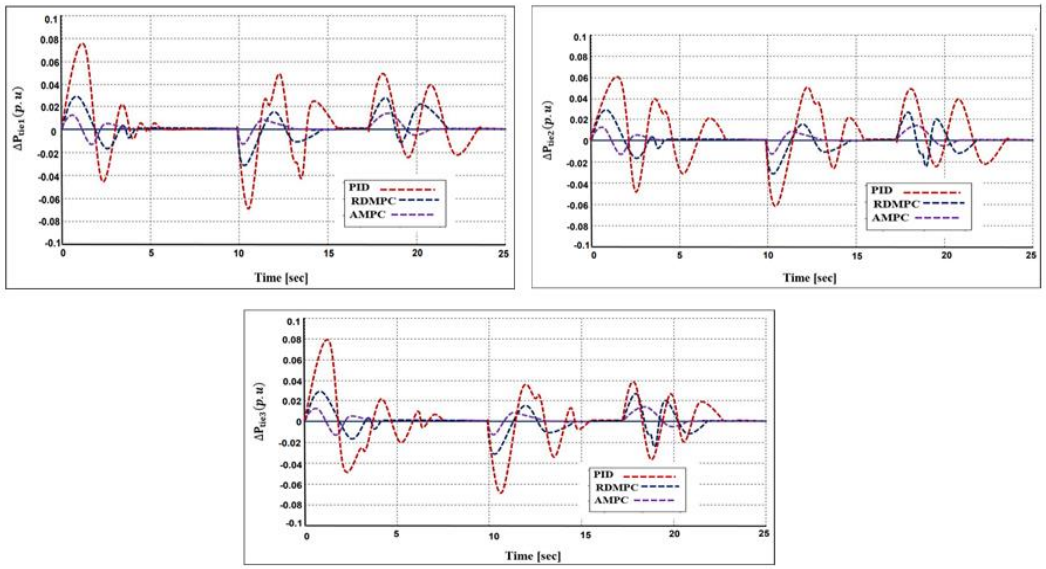

Figure 5-10 Tie-line active power deviations for area 1, 2 and 3 respectively

5.3.4 Case 4; Robustness test on parameter change T_G (two-area hydro-thermal power system)

The performance of the controller schemes are further demonstrated under two conditions of changing the thermal governor time T_G for a 60% increase and a 60% decrease. The control schemes PID, RDMPC, and AMPC was simulated for frequency deviation Δf_1, Δf_2 and Δf_3. Figure 5-11 and 5-12 shows the frequency response for a 60% increase and decrease in T_G

parameter variation and Table 5-2 and 5-3 show comparison indices and percentage improvement of AMPC on PID and RDMPC respectively. From the comparative analysis, there is 53.84%, 25.00% and 57.80% improvement on RDMPC in settling time, undershoot and peak overshoot respectively at 60% increased T_G in CA 1, similarly, with a 48.28%, 57.50% and 11.11% improvement on RDMPC in settling time, undershoot and peak undershoot when the system parameter is decreased by 60% T_G in CA 2. It is evidence that AMPC is more robust with a significant improvement over RDMPC and PID.

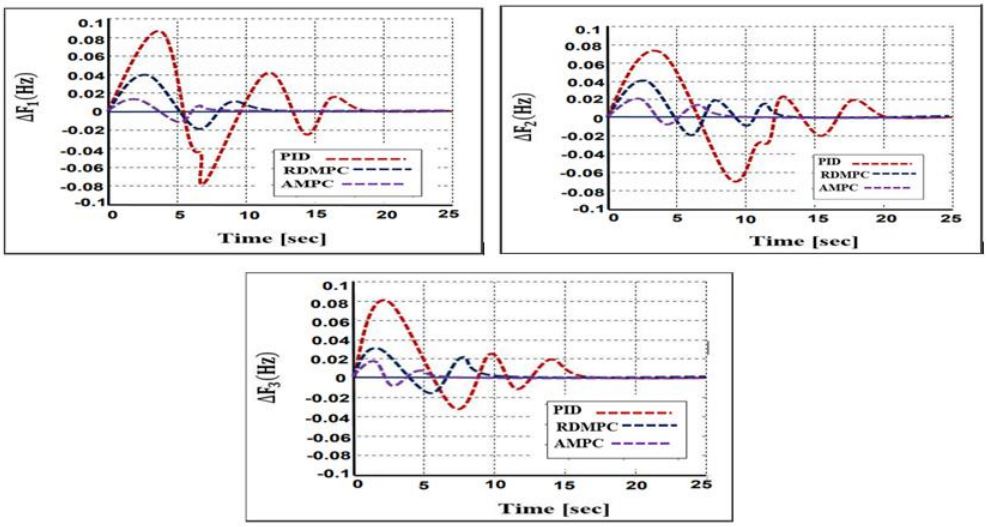

Figure 5-11 Frequency response for 60% increase in T_G parameter variation

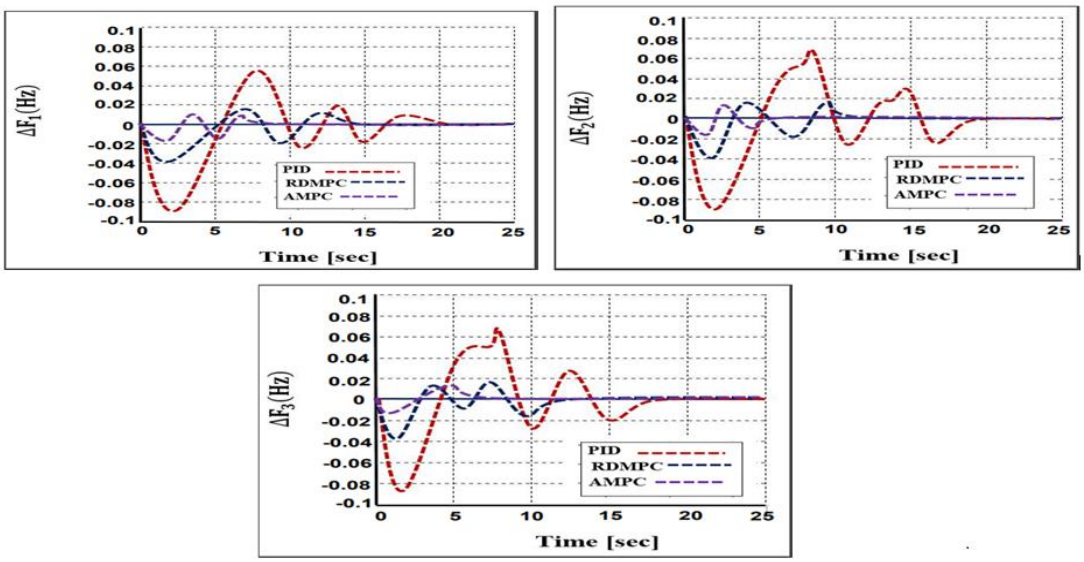

Figure 5-12 Frequency response for 60% decrease in T_G parameter variation

Table 5-3 Performance comparison for 60% Increase T_G parameter variation

System parameter	CA	60% Increase in T_G parameter variation			60% Decrease in T_G parameter variation		
		PID	RDMPC	AMPC	PID	RDMPC	AMPC
Setting time (s)	Δf_1	17.00	13.01	6.01	20.00	24.7	7.3
Undershoot (Pa.MW)	Δf_1	-0.08	-0.02	-0.0.15	-0.09	-0.04	-0.17
Peak overshoot (p.a MW)	Δf_1	0.085	0.04	0.017	0.055	0.018	0.018
Setting time (s)	Δf_2	19.01	14.00	7.02	19.00	12.01	5.6
Undershoot (Pa.MW)	Δf_2	-0.07	-0.022	-0.013	-0.08	-0.038	-0.015
Peak overshoot (p.a MW)	Δf_2	0.075	0.043	0.018	0.063	0.016	0.016
Setting time (s)	Δf_3	17.5	8.01	6.5	17.02	12.7	6.3
Undershoot (Pa.MW)	Δf_3	-0.03	-0.019	-0.015	-0.083	-0.04	-0.016
Peak overshoot (p.a MW)	Δf_3	0.084	0.035	0.018	0.07	0.018	0.017

Table 5-4 Improvement percentage of T_G parameter variation

System Parameter	CA	% Improvement of AMPC w.r.t PID & RDMPC			
		60% $>$ T_G w.r.t PID	60% $>$ T_G w.r.t RDMPC	60% $<$ T_G w.r.t PID	60% $<$ T_G w.r.t RDMPC
Setting time (s)	Δf_1	64.70	53.84	81.11	48.28
Undershoot (Pa.MW)	Δf_1	75.00	25.00	81.11	57.28
Peak overshoot (p.a MW)	Δf_1	80.00	57.50	67.27	11.11
Setting time (s)	Δf_2	63.07	49.86	70.53	53.37
Undershoot (Pa.MW)	Δf_2	81.42	40.91	81.25	60.52

Peak overshoot (p.a MW)	Δf_2	76.00	58.14	74.60	62.52
Setting time (s)	Δf_3	62.86	18.85	62.60	50.39
Undershoot (Pa.MW)	Δf_3	50.00	21.05	80.72	60.00
Peak overshoot (p.a MW)	Δf_3	78.57	48.57	75.71	5.556

5.3.5 Case 5; Downtime uncertainty (three -area hydro-thermal system)

In a load disturbance of 0.01 p.u, it is assumed that CA 3 is completely cut off for 5 s, i.e fails to operate due to downtime in the power plant, leaving CA 1 and CA 2 to participate in the LFC. Figures 5-13 to 5-15 shows dynamic response graph of Δf_1, Δf_2 , ACE_1, ACE_2 and ΔP_{tie} respectively, AMPC and RDMPC rapidly return the dynamic response to zero by satisfying all physical constraints, and closed-loop stability, despite the downtime in CA 2. Although PID returns the dynamic response to zero but with a high overshoot and settling time. AMPC displays a better control measure by fast-tracking the system dynamic oscillation to steady-state.

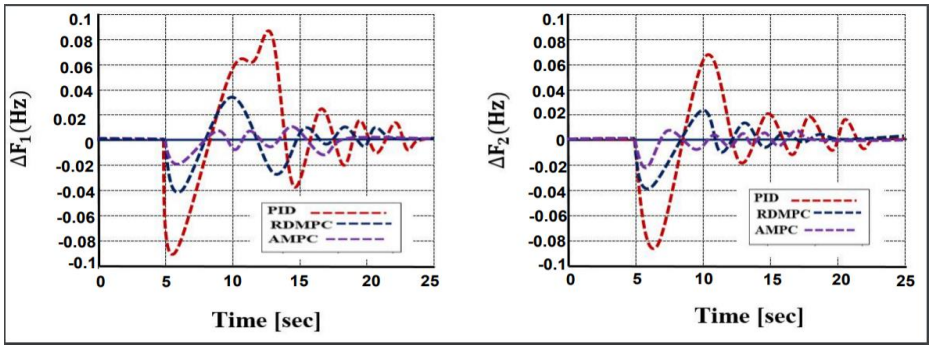

Figure 5-13 Frequency response with downtime uncertainty

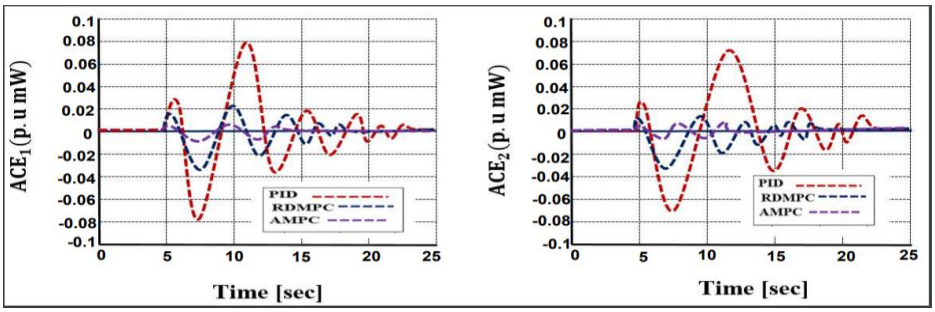

Figure 5-14 Area control error with downtime uncertainty

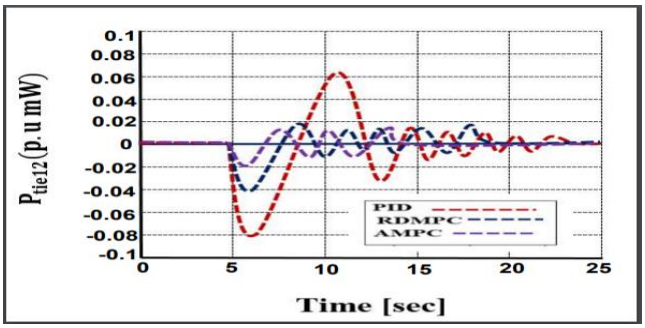

Figure 5-15 Tie line active power deviation with downtime uncertainty

5.4.6 Case 6; Non-linearity constraint (two-area hydro-thermal system)

Finally, simulation is done considering the effect of GRC and GDB performance in real-time systems. The power system model of hydro and thermal plant with included GRC and GDB is shown in Figure 5-16 and 5-17. In order to obtain accurate LFC, it is necessary to consider the effect of GRC and GDB on the performance of AMPC, RDMPC and PID. It is assumed that GRC of 10% p.u/min for reheat thermal system and a dead bank of ± 0.036 Hz as in [19]. Simulation is done only on the two-area hydro-thermal power system, this is because it has similar oscillation with the three-area network. Figure 5-18 shows the frequency deviation Δf_1, Δf_2 in CA 1 and CA 2 with nonlinear constraint, it is evidence that the dynamic response showed is highly oscillatory in the case of closed-loop GRC as compared with controllers without GRC. Table 5-3 show the comparison of the different controller including nonlinear constraints with the settling time, undershoot and peak undershoot are considerably high.

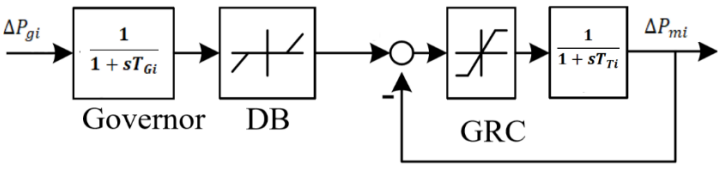

Figure 5-16 GRC and GDB in thermal power system

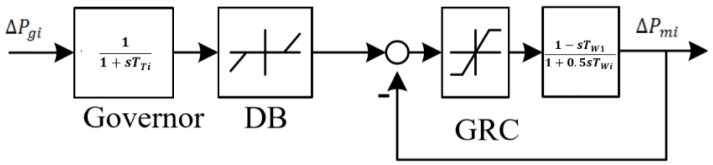

Figure 5-17 GRC and GDB in hydropower system

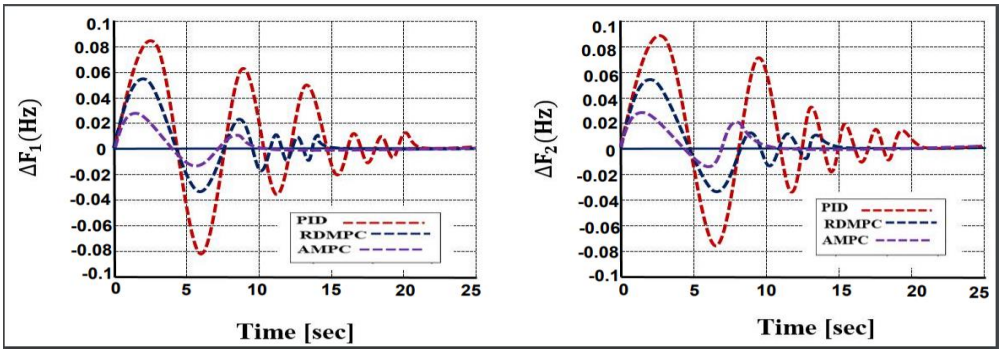

Figure 5-18 Frequency response in area 1 and area 2 with nonlinear constraint

Table 5-5 Comparison of the different controller including nonlinear constraints

System parameter		Close loop GRC

	CA	PID	RDMPC	AMPC
Setting time (s)	Δf_1	22.05	14.01	9.090
Undershoot (Pa.MW)	Δf_1	-0.080	-0.030	-0.018
Peak overshoot (p.a MW)	Δf_1	0.082	0.058	0.018
Setting time (s	Δf_2	21.03	15.00	11.08
Undershoot (Pa.MW)	Δf_2	-0.078	-0.038	-0.019
Peak overshoot (p.a MW)	Δf_2	0.083	0.077	0.030

5.5 Chapter conclusion

In this chapter, in addition to the RDMPC control algorithm, the AMPC method is proposed for the LFC control problem. The ideal was to investigate the effectiveness of AMPC control to improve on RDMPC performance results in chapter 4, to address dynamic parameter changes. The simulation results for two-area and three-area hydro-thermal systems show that the AMPC has better performance response when compared to PID and RDMPC algorithm in terms of dynamic and steady-state performance, in case of multiple load disturbance, parameters variation and nonlinearity. This work can be considered as an advancement to the knowledge contribution of MPC to the optimal LFC solution for IPS by developing AMPC to effectively improve the performance of RDMPC.

CHAPTER 6

CONCLUSION AND FUTURE RESEARCH

6.0 Conclusion

This dissertation proposed three different controllers scheme, the conventional PID, RDMPC and AMPC controller applied on two different power systems, two-area and three-area hydrothermal IPS. The power system is linearized using a mathematical model. The main objective is to effectively control frequency by maintaining its nominal value while keeping the tie line active power and ACE to zero. In chapter 4, RDMPC algorithm was developed as a convex optimization problem with linear matrix inequalities (LMI) and was compared with a conventional PID controller using MATLAB simulation on two-area and three-area hydrothermal power systems in the presence of frequency deviation and ACE. The simulation result shows that RDMPC significantly has a better dynamic response, while PID having a large setting time, undershoot and peak overshoot. This establishes the fact that MPC's are far better, more robust controllers than a conventional PID controller.

Despite the robust nature of RDMPC, the result shows some limitations of the system varying dynamics. Hence an adaptive MPC algorithm was developed, with expanded state vectors and rolling optimization to enhance online operational capability and speed of response for performance improvement over RDMPC. Simulation was done on two-area and three area power systems, in order to check the effectiveness of the AMPC controller. Robustness and comparative analysis are done in terms of transient response i.e., setting time, undershoot and peak overshoot between the proposed controller PID, RDMPC, and AMPC in the presence of frequency deviation, tie-line active power deviation, and ACE. The result shows the superiority of AMPC over RDMPC and PID with significant performance improvement. Generator rate constraint and governor dead bank were introduced to the system model. Despite the effect of nonlinearity constraint AMPC perform better compared to PID and RDMPC. The adaptive part uses an observer system that was designed and embedded within each subsystem controller to handle fast state estimations and operating conditions tracking. Fast reduction in computational burden and time coupled to the adaptive aspect makes it attractive for real-time and online implementation.

One of the main assumptions in this research is that all communication between all subsystems is reliable and possible failure in the communication network including delays were not put into consideration. During the formulation and tests, a controlled prediction horizon was used but the case of using longer prediction horizons was not exploited in this work to see the effect on stability and performance, possible future research can be done on the area. Finally, this dissertation achieved an MPC control structure that effectively deals with frequency mismatch errors, plant uncertainties, nonlinearity constraints with a very practical speed of response to these changes.

6.1 Future research remarks

The effect on subsystem performance in terms of robustness when there is communication failure from neighbour subsystems or measurement loss is not considered in this research. This will aid in the system reverting to an operational mode that is stable operating in decentralized mode until measurement data and interactions are restored. The suggestions offered by authors [1] and [2] for fault-control algorithms in their recent research can be adopted into DMPC, RDMPC and AMPC to cope with communication failures and measurement data loss.

The expected results that will be obtained from this recommendation and added to this work research will have a significant impact on the control of LFC as it will improve economic performance under uncertainties conditions and in the presence of model parameter uncertainties.

Also, to develop a model that will combine adaptive MPC with a robust DMPC for LFC for complex IPS should be considered for future research. To meet with the competitive demand for power system generation, transmission, and distribution.

APPENDIX A

A.1 Power system Parameters

Model, parameters and input variable used for the simulation of the two-area and three-area power systems.

Table A 3 Power system parameter variation

Parameter	Description	Unit
$\Delta f(t)$	Frequency disturbance	Hz
$\Delta P_m\,(t)$	Generator output power deviation	p.u. MW
$\Delta P_v(t)$	Governor valve position	p.u.
$\Delta P_{gi}(t)$	Governor valve servomotor position deviation	P.u.
$\Delta P_{tie}\,(t)$	Tie-line active power deviation	p.u.MW
$\Delta P_L\,(t)$	Load disturbance	p.u.MW
$\Delta\delta(t)$	Rotor angular distance	rad
K_P	Power gain	Hz/p.u.MW
K_{ri}	Reheat turbine gain	Hz/p.u.MW
T_P	Power system time out	s
T_w	Water starting time	s
T_1, T_2, T_R	Hydrothermal time constant	s
T_G	Thermal governor time	s
T_T	Turbine time constant	s
K_{Sij}	Interconnected gain between areas	p.u.MW/Hz
B_i	Frequency bias factor	Hz\ p.u.MW
R_i	Speed drop due to governor action	Hz\ p.u.MW
ACE	Area control error	p.u.MW

A.2 Power system Parameters and values

Table A 2 Parameters and variables values used in thermal and hydro power plants

Parameter 1	Values	Parameter 2	Values	Parameter 3	Values	Unit
T_{G1}	0.08	T_{G2}	0.8	T_{G3}	0.2	s
T_{P1}	20	T_{P2}	15	T_{P3}	15	s
B_1	0.425	B_2	0.494	B_3	0.38	p.u.MW/Hz
R_1	2.4	R_2	3.0	R_3	3	Hz/p.u.M
K_{P1}	120	K_{P2}	80	K_{P3}	110	Hz
Ts_{12}	0.545	Ts_{21}	0.545	Ts_{31}	0.545	p.u MW
K_{R1}	0.5	K_{R2}	0.5	K_{R3}	0.5	Hz/p.u.MW
T_{T1}	0.3	T_{T2}	48	T_{T3}	0.3	s
T_{R1}	10	T_{R2}	0.6	T_{R3}	10	s

REFERENCE

[1] Indranil Pan, and Saptarshi Das, “Fractional Order Load-Frequency Control of Interconnected Power Systems Using Chaotic Multi-Objective Optimization,” 1611.09802, 2015.

[2] P. Kundur, N. J. Balu, and M. G. Lauby, “Power system stability and control,” McGrawhill New York, 1994.

[3] Yesil, E. and M.G. Eksin, “Self tuning fuzzy PID type load and frequency controller,” Energ. Conversion Manage, 45: 377-390, 2004.

[4] K. Sabahi, A. Sharifi, M. Aliyari Sh., M Teshnehlab, M Aliasghary (2008), “Load Frequency Control in Interconnected Power System Using Multi-Objective PID Controller,” Journal of Applied Sciences, 8:36763682. DOI:10.3923, 2008.

[5] D. Kothari and I. Nagrath, “Power system engineering,” Tata McGraw-Hill, 2008.

[6] M. H. Kazemi, M. Karrari, and M. B. Menhaj, “Decentralized robust adaptive-output feedback controller for power system load frequency control,” Electrical Engineering (Archiv fur Elektrotechnik), vol. 84, no. 2, pp. 75–83, 2002.

[7] Y. Wang, R. Zhou, and C. Wen, “New robust adaptive load-frequency control with system parametric uncertainties,” in Generation, Transmission, and Distribution, IEE Proceedings-, vol. 141, no. 3, pp. 184–190, 1994.

[8] D.Q. Mayne, J.B. Rawlings, C.V. Rao, P.O.M. Scokaert, Constrained model predictive control: Stability and optimality, Automatica 36, 789–81, 2000.

[9] K. Lim, Y. Wang, and R. Zhou, “Robust decentralized load-frequency control of multiarea power systems,” in Generation, Transmission, and Distribution,” IEE Proceedings, vol. 143, no. 5, pp. 377–386, 1996.

[10] Z. Al-Hamouz, H. Al-Duwaish, and N. Al-Musabi, “Optimal design of a sliding mode AGC controller: Application to a nonlinear interconnected model,” Electric Power Systems Research, vol. 81, no. 7, pp. 1403–1409, 2011.

[11] G. Ray, A. Prasad, and T. Bhattacharyya, “Design of decentralized robust load frequency controller based on SVD method,” Computers & Electrical Engineering, vol. 25, no. 6, pp. 477–492, 1999.

[12] S. K. Aditya and D. Das, “Design of load frequency controllers using a genetic algorithm for two -area interconnected hydropower system,” Electric Power Components and Systems, vol. 31, no. 1, pp. 81–94, 2003.

[13] Z. Al-Hamouz and H. Al-Duwaish, “A new load frequency variable structure controller using genetic algorithms,” Electric Power Systems Research, vol. 55, no. 1, pp. 1–6, 2000.

[14] E. Çam and I. Kocaarslan, “A fuzzy gain scheduling PI controller application for an interconnected electrical power system,” Electric Power Systems Research, vol. 73, no. 3, pp. 267–274, 2005.

[15] D. Chaturvedi, P. Satsangi, and P. Kalra, “Load frequency control: a generalised neural network approach,” International Journal of Electrical Power & Energy Systems, vol. 21, no. 6, pp. 405–415, 1999.

[16] E. Ali and S. Abd-Elazim, “Bacteria foraging optimization algorithm-based load frequency controller for interconnected power system,” International Journal of Electrical Power & Energy Systems, vol. 33, no. 3, pp. 633–638, 2011.

[17] I. Kocaarslan and E. Çam, “Fuzzy logic controller in interconnected electrical power systems for load-frequency control,” International Journal of Electrical Power & Energy Systems, vol. 27, no. 8, pp. 542–549, 2005.

[18] K. Sabahi, M. Teshnehlab, and others, “Recurrent fuzzy neural network by using feedback error learning approaches for LFC in interconnected power system,” Energy Conversion and Management, vol. 50, no. 4, pp. 938–946, 2009.

[19] Surya Prakash1, S. K. Sinha, “Application of artificial intelligence in load frequency control of interconnected power system,”. International Journal of Engineering, Science and Technology Vol. 3, No. 4, pp. 264-275, 2011.

[20] Aravindan P., Sanavullah M.Y, “Fuzzy Logic Based Automatic Load Frequency Control of Two Area Power System with GRC,” International Journal of Computational Intelligence Research, Volume 5, Number 1. pp. 37–44, 2009.

[21] Talaq J., Fadel A.l., Basri, “Adaptive Fuzzy gain scheduling for Load Frequency Control, IEEE Transaction on Power System,” Vol.14, No.1, pp.145-150, 1999.

[22] N.Ibraheem, P. Kumar and D.P. Kothari, “Recent philosophies of automatic generation control strategies in power systems”, IEEE Power Syst., Vol. 20, no. 1, pp. 346-357, 2005.

[23] Sachin C. Patwardhan, “An Introduction to Model Predictive Control TEQIP Workshop,” IIT Kanpur 22’nd Sept. 2016.

[24] Orukpe P, E., “Model Predictive Control Fundamentals,” Nigerian Journal of Technology (NIJOTECH) Vol. 31, No. 2, pp. 139, ISSN 1115-8443, 2012.

[25] Aswin N. Venkat, “Distributed Model Predictive Control,” Theory and Applications, Phddesertations, University of Wisconsin, 2006.

[26] C. Hajiyev and H. E. Soken, “Robust adaptive unscented Kalman filter for attitude estimation of pico satellites,” Int. J. Adapt. Control Signal Process., vol. 28, no. 2, pp. 107–120, 2014.

[27] E. Camacho and C. Bordons, “Model Predictive Control,” Springer, Berlin, second edition, 2004.

[28] M. Morari and J. H. Lee, “Model predictive control: past, present, and future” In Proceedings of joint 6th international symposium on process systems engineering (PSE ’97) and 30th European symposium on computer aided process systems engineering (ESCAPE 7), Trondheim, Norway, 1997.

[29] S. J. Qin and T. A. Badgwell, “A survey of industrial model predictive control technology,” Control Engineering Practice, 11(7):733–764, 2003.

[30] Amita Singh, Veena Sharma, Preeti Dahiya and Ram N. Sharma, “Model Predictive Based Load Frequency Control of Interconnected Power Systems,” Recent Advances in Electrical & Electronic Engineering, 11, 322-333, 2018.

[31] A. N. Venkat, "Distributed model predictive control," Theory and applications. Ph.D. thesis, Department of Chemical and Biological Engineering, University of Wisconsin, 2006.

[32] Al-Gherwi, W., Budman, H., and Elkamel, A. "An online algorithm for robust distributed Model Predictive Control," Proceedings of the Advanced Control of Chemical Processes ADCHEM, Paper no. 33, Turkey, 2009.

[33] Li, S., Zhang, Y., and Zhu, Q. "Nash-optimization enhanced distributed model predictive control applied to the shell benchmark problem," information science, 170, 329-349, 2005.

[34] Lunze, Jan "Feedback control of large-scale systems," Prentice Hall, London, UK, 1992.

[35] Rawlings, James B., and Stewart, Brett T. "Coordinating multiple optimizations based controllers: new opportunities and challenges", Journal of Process Control, 18, 839-845, 2008.

[36] Scattolini, R., "Architecture of distributed and hierarchical model predictive control – A review", Journal of Process Control, 19, 723-731, 2009.

[37] V. Havlena and J. Lu, "A distributed automation framework for plant-wide control, optimization, scheduling, and planning," In Proceedings of the 16th IFAC World Congress, Prague, Czech Republic, 2005.

[38] M. Katebi and M. Johnson, "Predictive control design for large-scale systems," Automatica, 33: 421–425, 1997.

[39] B. A. Ogunnaike and W. H. Ray. Process Dynamics, "Modeling, and Control," Oxford University Press, New York, 1994.

[40] G. Zhu, M. Henson, and B. Ogunnaike, "A hybrid model predictive control strategy for nonlinear plant-wide control," Journal of Process Control, 10:449–458, 2000.

[41] T. Keviczky, F. Borelli, and G. J. Balas, "Stability analysis of decentralized RHC for decoupled systems," In Proceedings of the Joint 44th IEEE Conference on Decision and Control and European Control Conference, pages 1689–1694, Seville, Spain, 2005.

[42] W. B. Dunbar and R. M. Murray, "Distributed receding horizon control with application to multi-vehicle formation stabilization," Automatica, 2(4):549–558, 2006.

[43] A. Richards and J. How, "A decentralized algorithm for robust constrained model predictive control," In Proceedings of the American Control Conference, Boston, Massachusetts, 2004.

[44] D. Jia and B. H. Krogh, "Distributed model predictive control," In Proceedings of the American Control Conference, pages 2767–2772, Arlington, Virginia, 2001.

[45] E. Camponogara, D. Jia, B. H. Krogh, and S. Talukdar, "Distributed model predictive control," IEEE Control Systems Magazine pages 44–52, 2002.

[46] N. Motee and B. Sayyar-Rodsari, "Optimal partitioning in distributed model predictive control," In Proceedings of the American Control Conference, pages 5300–5305, Denver, Colorado, 2003.

[47] L. Magni and R. Scattolini, "Stabilizing decentralized model predictive control of nonlinear systems," Automatica, 42(7):1231–1236, 2006.

[48] N. R. Sandell-Jr., P. Varaiya, M. Athans, and M. Safonov, “Survey of decentralized control methods for larger-scale systems,” IEEE Transactions on Automatica Control, 23(2):108–128, 1978.

[49] H. Cui and E. Jacobsen, “Performance limitations in decentralized control,” Journal of Process Control, 12:485–494, 2002.

[50] Morari, M., and Zafiriou, E. “Robust process control”, Prentice Hall, NJ, USA, 1989.

[51] Kothare, M., Balakrishnan, V., and Morari, M, “Robust constrained model predictive control using linear matrix inequalities”, Automatica, 22 (10), 1361-1379, 1996.

[52] Löfberg, J, “YALMIP: A toolbox for modeling and optimization in MATLAB,” In Proceedings of the CACSD Conference, Taipei, Taiwan, 2004.

[53] VanAntwerp, J.G. and Braatz, R.D., “A tutorial on linear and bilinear matrix inequalities”, Journal of Process Control, 10, 363-385, 2000.

[54] Boyd, S., El.Ghaoui, L., Feron, E., and Balakrishnan, V., “Linear matrix inequalities in system and control theory,” SIAM, USA, 1994.

[55] Pistikopoulos, E., Georgiadis, M, and Dua, V., “Multi-Parametric model-based control,” Wiley-VCH, 2007.

[56] Bemporad, A., Morari, M., Dua, V., and Pistikopoulos, N. (2002) “The explicit linear quadratic regulator for constrained systems,” Automatica, 38, 3-20.

[57] Chu, D., “Explicit robust model predictive control and its applications,” Ph.D. thesis, University of Alberta, Edmonton, Canada, 2006.

[58] Al-Gherwi, W., Budman, H., and Elkamel, A., “Robustness issues related to the application of distributed model predictive control strategies,” Proceedings of the 17th World Congress IFAC, Seoul, Korea, 8395-8400, 2008.

[59] Xiangjie Liu,Yi Zhang ,Kwang Y. Lee,"Robust distributed MPC for load frequency control of uncertain power systems,"Department of Electrical and Computer Engineering, Baylor University, TX 76798-7356, USA,0967-0661,2016.

[60] Liuping Wang, “Model Predictive Control System Design and Implementation Using MATLAB®”, Advances in industrial control, ISBN 978-1-84882-330-3, e-ISBN 978-1-84882-331-0, DOI 10.1007/978-1-84882-331-0, Advances in Industrial Control ISSN 1430-9491, 2009

[61] Al-Gherwi, W., Budman, H., and Elkamel, A., “An online algorithm for robust distributed Model Predictive Control,” Proceedings of the Advanced Control of Chemical Processes ADCHEM, Paper no. 33, Turkey, 2009.

[62] Guo-Qiang Zeng, Xiao-Qing Xie and Min-Rong Chen, “An Adaptive Model Predictive Load Frequency Control Method for Multi-Area Interconnected Power Systems with Photovoltaic Generations”, 10, 1840; doi:10.3390/en10111840, Energies 2017.

[63] XiaokangXu, Jun Peng, Rui Zhang, Bin Chen, Feng Zhou, Yingze Yang, Kai Gao, and Zhiwu Huang, “Adaptive Model Predictive Control for Cruise Control of High-Speed Trains with Time-Varying Parameters”, Journal of Advanced Transportation, Article ID 7261726, 2019.

[64] D. G. Lainiotis, K. Plataniotis, M. Papanikolaou, and P. Papaparaskeva, “Discrete Riccati equation solutions: Distributed algorithms,” Mathematical Problems in Engineering, 2:319–332, 1996.

[65] M. K. Sundareshan and R. M. Elbanna. Design of decentralized observation schemes for largescale interconnected systems: Some new results. Automatica, 26(4):789–796, 1990.

[66] M. Saif and Y. Guan, "Decentralized state estimation in large-scale interconnected dynamical systems," Automatica, 28(1):215–219, 1992.

[67] N. Viswanadham and A. Ramakrishna, "Decentralized estimation and control for interconnected systems," Large Scale Systems, 3:255–266, 1982.

[68] C. R. Cutler and B. L. Ramaker, "Dynamic matrix control—a computer control algorithm," In Proceedings of the Joint Automatic Control Conference, 1980.

[69] J. Richalet, A. Rault, J. L. Testud, and J. Papon, "Model predictive heuristic control: Applications to industrial processes," Automatica, 14:413–428, 1978.

[70] K. R. Muske and T. A. Badgwell, "Disturbance modeling for offset-free linear model predictive control," Journal of Process Control, 12(5):617–632, 2002.

[71] Xiangjie Liu,1 HuiyunNong, Ke Xi, and Xiuming Yao, "Robust Distributed Model Predictive Load Frequency Control of Interconnected Power System," Hindawi Publishing Corporation Mathematical Problems in Engineering, Article ID 468168, 10 pages http://dx.doi.org/10.1155/2013/468168, 2013.

[72] M. V. Kothare, V. Balakrishnan, and M. Morari, "Robust constrained model predictive control using linear matrix inequalities," Automatica, vol. 32, no. 10, pp. 1361–1379, 1996.

[73] X. Liu, S. Feng, and M. Ma, "Robust MPC for the constrained system with polytopic uncertainty," International Journal of Systems Science, vol. 43, no. 2, pp. 248–258, 2012.

[74] H. Shayeghi, H. A. Shayanfar, and O. P. Malik, "Robust decentralized neural networks based LFC in a deregulated power system," Electric Power Systems Research, vol. 77, no. 3-4, pp. 241–251, 2007.

[75] A. N. Venkat, I. A. Hiskens, J. B. Rawlings, and S. J. Wright, "Distributed MPC strategies with application to power system automatic generation control," IEEE Transactions on Control Systems Technology, vol. 16, no. 6, pp. 1192–1206, 2008.

[76] T. H. Mohamed, H. Bevrani, A. A. Hassan, and T. Hiyama, "Decentralized model predictive based load frequency control in an interconnected power system," Energy Conversion and Management, vol. 52, no. 2, pp. 1208–1214, 2011.

[77] K. Vrdoljak, N. Peric, and I. Petrovi, "Sliding mode based load frequency control in power systems," Electric Power Systems Research, vol. 80, no. 5, pp. 514–527, 2010.

[78] Jianping Guo, Lili Dong, "Sliding Mode Based Load Frequency Control for an Interconnected Power System with Nonlinearities," under review, submitted to International Journal of Intelligent Control and Systems, 2015.

[79] Jianping Guo, "Load Frequency Control of a Two Area Power System with Non-reheat Turbines by SMC Approach," accepted by Journal of Energy and Power Engineering, to be published on June 30, 2015.

[80] P. Kundur, Power System Stability, and Control, McGraw-Hill Inc, 1993.

[81] H. Golpira and H. Bevrani, "Application of GA optimization for automatic generation control in realistic interconnected power system," in Proceedings of International Conference on Modeling, Identification and Control, Okayama, Japan, pp. 30-34, 2010.

[82] R. Francis and I. A. Chidambaram, “Control performance standard based load frequency control of a two area reheat interconnected power system considering governor dead band nonlinearity using fuzzy neural network,” International Journal of Computer Applications, vol. 46, no. 15, pp. 41-48, 2012.

[83] J. P. Lee and H. G. Kim, “Application of FESS controller for load frequency control,” Journal of International Conference on Electric Machines and System, vol. 2, no. 3, pp. 361-366, 2013.

[84] A. M. Yousef, J. A. Khamaj and A. S. Oshaba, “Steam hydraulic turbines load frequency controller based on fuzzy logic control,” Research Journal of Applied Sciences, Engineering and Technology, vol. 4, no. 15, pp. 2375-2381, 2012.

[85] O. I. Elgerd, “Control of Electric Power System,” Department of Electrical Engineering, University of Florida, Gainesville, Florida, Technical Report.

[86] G. Panda, S. Panda and C. Ardil, “Automatic generation control of interconnected power system with generation rate constraints by hybrid neuro fuzzy approach,” International Journal of Electrical and Electronics 90 Engineering, vol. 3, no. 9, pp. 532-537, 2009.

[87] D. Kothari and I. Nagrath, Power System Engineering, 2nd ed. New York: McGRAW-Hill, 2008.

[88] S. R. Khuntia and S. Panda, “Simulation study for automatic generation control of a multi-area power system by ANFIS approach.” Applied Soft Computing, vol. 12, no. 1, pp. 333-341, 2012.

[89] North American Electric Corporation, “Frequency Response Initiative Report,” Atlanta, GA, Tech. Report, 2012.

[90] Amit Panwar, Sunita Chahar, “Automatic Load Frequency Control of Three Area Power System Using Artificial Intelligence," 978-1-5090-3411-6/16, 2016 IEEE, DOI 10.1109/ICMETE.58, International Conference on Micro-Electronics and Telecommunication Engineering, 2016.

[91 H. Michalska, D.Q. Mayne, Robust receding horizon control of constrained nonlinear systems, IEEE Transactions on Automatic Control 38 ,11,1623–163, 1993.

[92] Veronica Adetola, Darryl DeHaanb, Martin Guay, “Adaptive model predictive control for constrained nonlinear systems,” Systems & Control Letters 58 320–326, 2009.

[93] Ramakrishna Raghutu, P V Ramanarao, “ADAPTIVE PREDICTIVE LOAD FREQUENCY CONTROL OF A MICROGRID”, International Journal of Mechanical Engineering and Technology (IJMET) Volume 9, Issue 4, pp. 960–970, Article ID: IJMET_09_04_109, 2018.

[94] Monimoy Bujarbaruah, Xiaojing Zhang, Ugo Rosolia, Francesco Borrelli, “Adaptive MPC for Iterative Tasks”, 2018 IEEE Conference on Decision and Control (CDC) 1804-0983, 2018.

[95] Xiaokang Xu, Jun Peng, Rui Zhang, Bin Chen, Feng Zhou, Yingze Yang, Kai Gao, and Zhiwu Huang, “Adaptive Model Predictive Control for Cruise Control of High-Speed Trains with Time-Varying Parameters,” Journal of Advanced Transportation, Article ID 7261726, Volume 2019.

[96] Adelhard Beni Rehiara, He Chongkai, Yutaka Sasaki, Naoto Yorino, and Yoshifumi Zoka, “An Adaptive IMC-MPC Controller for Improving LFC Performance,” 978-1-5386-4950-3/17/$31.00 © IEEE, 2017.

[97] Mhaskar, P., “Robust model predictive control design for fault-tolerant control of process systems,” Industrial & Engineering Chemistry Research, 45, 8565-8574, 2006.

[98] Gandhi, R. and P. Mhaskar "A safe-parking framework for plant-wide fault tolerant control," Chemical Engineering Science., 64, 3060-3071, 2009.